Norwegian University
of Life Sciences

Master's Thesis 2020 30 ECTS
Faculty of Environmental Sciences and Natural Resource Management
(MINA)

Predicting the Extent of Root and Butt Rot in Stems of Norway Spruce (*Picea abies*)

Ole Marius Tollefsen Moen
M.Sc. Forest Sciences

Acknowledgements

I would like to thank my supervisors Professor Terje Gobakken and Professor Hans Fredrik Hoen for their patience and help throughout the whole process of this thesis. Professor Hans Fredrik Hoen formulated the thesis. Professor Terje Gobakken has been extremely helpful and I feel grateful for the opportunity to work with him. I would also like to extend my gratefulness to Dr. Ole Martin Bollandsås for invaluable help with statistics and modelling, Roar Økseter for help with equipment, Knut Finstad for making OptApt available, and Knut Nysveen and the Råheim-family for their hospitality when acquiring the field data.

This work was supported by the Research Council of Norway under the project «Precision forestry for improved resource utilization and reduced wood decay in Norwegian forests (PRECISION)» (NFR Project No. 281140). Without the support, the field work in this thesis could not have been conducted.

Abstract

Commercially, Norway spruce (*Picea abies* (L.) Karst) is the most important tree species in Norway, representing 72% of the industrial timber volume sold in 2019. However, Norway spruce is particularly prone to infection of root and butt rot pathogens, degrading the value of the resource. Studies using National Forest Inventory Data (NFI) show that the nationwide rot frequency of Norway spruce is somewhere between 7.9-9.5%. Other studies have indicated that the presence of root and butt rots are in proportions of approximately 1 out of 5 Norway spruce trees. Root and butt rots cause substantial annual economic losses estimated at NOK 100 millions. The losses are related to degradation of timber resources, per instance, culled by the harvester operator. However, the extent of which the root and butt rots develops up the stem is not known by the harvester operator. Therefore, developing a practical prediction model for rot heights in Norway spruce, to guide the operator in decision making, was addressed in this thesis.

The data sampling was carried out on three different occasions. In the first sampling, root and butt rot infected spruce trees were identified. Secondly, the trees were cut to examine the extent of rot in the stems. At last, tree-specific measurements were gathered.

The prediction model could explain approximately 21% of the variance in the dataset. Individually, the independent variables diameter at root, proportion of rot and tree height, showed a positive relationship to the prediction of rot height, with increasing values increasing the prediction of rot height. In the evaluation of the prediction model using optimal bucking, a total utilization grade of 76% was discovered. On tree level, the utilization grade was 74% with a standard error of 18%.

Sammendrag

Gran (*Picea abies* (L.) Karst) er det kommersielt viktigste treslaget i Norge, med en andel på 72 % av det industrielle tømmervolumet som ble solgt i 2019. Imidlertid er gran spesielt utsatt for rotråtesopper, som reduserer verdien av virket. Studier basert på data fra Landsskogtakseringer viser at den nasjonale råtefrekvensen i gran i Norge ligger et sted mellom 7.9-9.5 %. Andre studier har vist at omtrent 1 av 5 grantrær er infisert med rotråte. Uavhengig av hvor stor andelen faktisk er, forårsaker råte et estimert verditap på omkring 100 millioner norske kroner årlig. Disse tapene kommer som en følge av reduksjon av virkesverdier, blant annet når en hogstmaskinfører må bulte deler av en stamme. Når hogstmaskinføreren bulter, er det uvisst hvor langt rotråten strekker seg oppover i stammen. Derfor er det behov for en praktisk prediksjonsmodell som kan hjelpe til i prosessen med å håndtere gran med rotkjuke eller honningsopp. Å utvikle denne modellen var hovedmålsettingen med denne studien.

Data ble samlet i tre omganger. I første omgang ble grantrær med rotråte lokalisert. Deretter ble trærne kappet for å undersøke omfanget av råte i stammene. Til slutt ble tre-spesifikk informasjon samlet inn.

Prediksjonsmodellen forklarte 21 % av variansen i datasettet. Hver for seg viste de individuelle variablene rotdiameter, råteandel og trehøyde en positiv korrelasjon med råtehøyden, hvor økte verdier i de individuelle variablene resulterte i økte prediksjoner for råtehøyden. Under vurderingen av prediksjonsmodellen basert på optimal aptering, viste det seg at den totale apteringsgraden den oppnådde var på 76 %. På trenivå, var apteringsgraden 74 % med et standardavvik på 18 %.

Table of Contents

1. Introduction

1.1 Background

In an everchanging debate on climate changes, the forest industry has been enumerated as having a key role in Norway. The industry has potential in developing and accomplishing a more sustainable and climate friendly society, underlining the importance of increased utilization of forest resources (Ministry of Agriculture and Food, 2015). Its key role is through storage and absorption of carbon dioxide (CO2) from the atmosphere, thereby contributing to the global carbon cycle. Nationally, net absorption of greenhouse gasses in forests is 54% of all emissions from other sectors (Tomter & Dalen, 2018).

In Norway, 37.4% of the land area is covered by forests, representing a total standing volume under bark of 974 million m^3 (Statistisk Sentralbyrå, 2019). The total industrial timber volume sold in 2019 was 11.017 million m^3, resulting in a gross income of NOK 4.800 billion. Approximately 72% of the volume consisted of Norway spruce (*Picea abies* (L.) Karst), emphasizing its significant economic importance (Statistisk Sentralbyrå, 2020). Among other products, the specie is of economic importance in solid wood for timber construction and pulpwood for paper (Cadullo et al., 2016). However, the maximum economic potential of the good is absent due to biotic factors such as rot, for which it is particularly prone. Forest owners and the forest industry in general experience annual estimated losses of approximately NOK 100 million due to rot (Solheim, 2010).

1.2 Rot

Rot is decomposition of organic material due to fungal decay. The fungi produce enzymes which attacks the components of the wood. Categorization of rot is dependent on the position of decay and the decomposition of the components in the wood. The three main components in wood is cellulose, hemicellulose and lignin. The main rot categories in living trees are white-rot, which is most common in deciduous wood, and brown-rot, which is most common in coniferous wood (Bøhmer & Aarnes, 2017; Ryvarden, 2019; Solheim, 2010). White-rot decomposes all important components in the cellular wall. Normally, white-rot decomposes lignin and hemicellulose firstly, and cellulose after that, resulting in a light-colored fibrous material. Brown-rot, which decomposes the cellulose and hemicellulose, is typically brown (Mester et al., 2004; Solheim, 2010). Furthermore, rot can also be categorized on the position of decay in living trees. Hereunder, the two types of rot are stem rot and root rot. Stem rot, as the name suggest, appears in the stem itself. Root rot on the other hand, can further be divided into two sub-categories: root rot and butt rot. Real root rots stay in the root system, whereas butt rot can develop further up the tree (Solheim, 2010).

Rot is a substantial problem for the forest sector in Norway and specially for its most important specie, Norway spruce, hereafter referred to as spruce (Stamnes et al., 2000). Huse (1983) examined increment borer data from the Norwegian National Forest Inventory (NFI) from the period 1964-1976. The result indicated that 7.9% of the spruce trees were infected with rot. A similar study by Granhus and Hylen (2016) using NFI data from 1986-2004 showed a rot frequency of 9.5%. In 1992, a nation-wide stump study on spruce was performed in Norway. The results show that 26.8% of all the stumps were infected with root and butt rot. In this study, the two main root and butt rot pathogens were *Heterobasidion parviporum* Niemelä & Korhonen and fungi from the *Armillaria* spp. complex which individually and in combination appeared on 71% of the rotten stumps. Individually, *H. parviporum* was the most common pathogen approximately appearing on 16% of all stumps. *Armillaria* spp. was the second most common which appeared on approximately 5% of all stumps. Other rot types only accounted for around 3% of the total number of stumps (Huse et al., 1994). In his publication, Solheim (2010) supported the importance of these two root and butt rots in Norway. Thor et al. (2005) also informed that the main cause for economic losses due to root rot pathogens in the northern temperate zone are *Heterobasidion* spp. (*Heterobasidion annosum* (Fr.) Bref. s. Lato) and *Armillaria* spp.

1.2.1 *Heterobasidion* spp.

The *Heterobasidion* spp. complex are white rots. There is two types of root rot pathogens from this complex in Norway, *Heterobasidion Parviporum* and *Heterobasidion Annosum* (*Heterobasidion Annosum* sensu stricto) (Granhus & Hylen, 2016; Solheim, 2010). Differentiation is based on the host tree and distribution area. *H. Parviporum* is mainly detected on spruce, whereas *H. Annosum* primarily infects Scots pine (*Pinus sylvestris* L.), but can be found on spruce as well as deciduous trees (Hanssen et al., 2019). The primary channel for spreading is through the air, where propagules (mainly basidiospores) attach to freshly exposed wood surfaces. For instance, on damaged roots or stumps. After the pathogen has infected trees in an area or stand, a secondary source of infection can take place in healthy trees. Because the pathogen is not able to grow freely in the soil, this is through physical contact of the mycelium, through root contact or grafts (Garbelotto & Gonthier, 2013). As part of the primary infection channel, fruit bodies can originate on the lower part of stumps or in the root systems. Fruit bodies, which can exist for years, can produce spores when the temperature is above 0 degrees Celsius. In the root system of stumps, *Heterobasidion* spp. can live as long as 30-40 years, thereby inflicting danger of infection for the new generation of plants. The speed and rate of infection will vary with the spatial distribution of trees (Hanssen et al., 2019). The pattern and course of the disease in the tree relies on its age. Trees with ages up to 35 years can experience acute and critical infection resulting in death. Due to less resistant ability through lesser volume, the pathogen will more easily conquer smaller trees. On the other hand, older trees can experience a chronical disease cycle over a longer period of time. Generally, the rot will spread from the roots and upwards to the stem (Solheim, 2010). In Norway, *H. Parviporum* exists from Agder county to Saltfjellet in Nordland county. *H. Annosum* is most common in the western parts of the country to the north-western parts, however, it is discovered in the southern parts of the country as well as the eastern part (Hanssen et al., 2019). Hereafter, fungi from this complex will be referred to as *Heterobasidion* spp.

1.2.2 *Armillaria* spp.

There are four types of root rot pathogens from the *Armillaria* spp. complex in Norway, where *Armillaria borealis* and *Armillaria cepistipes* are the most common (Keča & Solheim, 2011). *Armillaria* spp. can be found on all tree species, and the two most common in Norway have the same behavioral pattern in forests. They are not considered as acting aggressively, however, they can establish on stressed trees (Hanssen et al., 2019). Risbeth (1985) states that the infection cycle starts with spore dispersal. *Armillaria* spp. are saprogenic and the main channel for infection is through rhizomorphs (mycelial cords) which develop in the ground. Rhizomorphs spread throughout dead and damaged roots (Solheim, 2010). In Hanssen et al. (2019) it is stated that smaller trees may die from infection. Solheim (2010) confirms and adds that the process is longer for larger trees. *A. borealis* is discovered throughout the country up to the county of Troms and Finnmark, whereas *A. cepistipes* is most common in the southern and central parts of the country (Keča & Solheim, 2011). Hereafter, fungi from this complex will be referred to as *Armillaria* spp.

1.2.3 Root and butt rot characteristics and implications for harvester operators

Symptoms of *Heterobasidion* spp. in living trees are in most cases not possible to distinguish from other root and butt rot pathogens (Asiegbu et al., 2005). However, in the cross-section of stumps, the characteristics may appear more distinctly. In the center, brown-toned color appears before turning brighter. In the decay, black spots of millimeter length embraced by white zones of cellulose appears. On the outside of the decay, a reaction zone of olive or green color against healthy wood is created (Solheim, 2010). *Armillaria* spp. can exist inside trees for years without observable symptoms. Symptoms are first identifiable after felling, and may appear with the same characteristics as *Heterobasidion* spp. Due to bacteria and other fungi interplaying in the process, the decay can appear with a more thorough blackness. Characteristics may also include a hollow space in the center of the stem, after the dissipation of lignin and cellulose (Solheim, 2010). In living trees, visual detection of root and butt rot may be indicated by needle loss or fruit bodies of the fungi. In addition, resin extrusion on severely infected trees can occur. The symptoms may be challenging or impossible to detect visually (Vollbrecht & Agestam, 1995). A study from Estonia on visual detection of root and butt rot discussed that a notable portion of visually categorized healthy trees in fact were affected. As a conclusion, it was stated that the visual inspection was not reliable (Allikmäe et al., 2017). In their study, Giordano et al. (2015) found an underestimation of rot (including *Heterobasidion* spp. and *Armillaria* spp.) from visual assessment compared to molecular methods of more than 90%. Axmon et al. (2004) argue that the difficulty of the visual inspection of root or butt rot in spruce is because of similarities in characteristics between rot and other factors, per instance cracks or dead spots of inner bark. As inspection through field registrations in the aforementioned studies is classified as challenging, a harvest machine operator is working in a stressing environment with managing controls and reduced view from the cab (Gellerstedt, 2002). The study found that harvester operators are managing as much as 4,000 control inputs per hour. In addition, the operator has trouble detecting root and butt rot. In Ostovar et al. (2019), it is stated that the current practice for harvester operators is to detect the presence of root and butt rot at the first felling cut of a tree. The detection is based on the changing color of the sawdust that originates from the cut. Thereby, the operator handles the boom to enable a visual examination of the stem, and to assess the extension of rot before cutting the stem to different assortments. With more handling of stems due to rot, economic losses through increased harvesting costs may appear (Hylen & Granhus, 2018; Seifert, 2007).

1.3 Evaluation of rot in Norway and implications for assortments

In Norway, a legislation determines that all marketable wood has to be measured (Skogbrukslova, 2005). The impartial and objective section of the measurement is conducted by Norsk Virkesmåling, which creates a neutral settlement between buyer and seller (Norsk Virkesmåling, n.d.-a). Norsk Virkesmåling is operating with different protocols for measuring wood. Hereunder are automatic measurement of length and diameter in assistance of manual sorting of qualities and dimensions, load measurement where length, width and height are used for estimation of the volume and quality, and photo-web measurement which does not require an employee to be present (Norsk Virkesmåling, n.d.-b). In addition to handling wood that is inbound between buyer and seller, control measurements are also conducted. Here proportions of the delivery are set aside for extensive examination by an employee. There are guidelines for handling of rot in sawn timber and pulpwood, and the latest publicly available were published in 2015 (Norsk Virkesmåling, 2015a; Norsk Virkesmåling, 2015b). In the guidelines for sawn timber, rot is not tolerated in any assortment. However, a maximum shortening of 60 cm is allowed on the log for clearing of rot, although, this reduces it to the second ranked grade (Norsk Virkesmåling, 2015b). In pulpwood, bright rot with approximately the same color as healthy wood is not considered as a fault. However, for darker decays, first grade pulpwood accepts up to 50% of the diameter or 25% of the surface area. For second grade pulpwood, up to 70% of the diameter and 50% of the surface area is accepted (Norsk Virkesmåling, 2015a).

Stems are cut into logs according to price lists. The price itself is calculated per cubic meter, dependent upon log quality, length and diameter (Øvrum & Vestøl, 2009). In accordance with the aforementioned standards from Norsk Virkesmåling for sawn timber, the presence of rot will enable shortening or declassification of the logs, and thereby reduce the value. Decay caused by *Heterobasidion* spp. will reduce the proportion of sawn timber and cause economical losses due to decay in the most valuable part of the stem, the butt end (Seifert, 2007). As the rot colonize, it will move upwards in the stem (Stamnes et al., 2000). Degradation of sawn timber can occur, where significant parts of the stem may be categorized as lower grade pulpwood or bioenergy (Hylen & Granhus, 2018). Rot height of *Heterobasidion* spp. in Norway spruce has been recorded as high as 10-12 meters up the stem, whereas *Armillaria* spp. seldom is over 2 meters (Hanssen et al., 2019; Stamnes et al., 2000; Stenlid & Redfern, 1998). A study by Tamminen (1985) recorded an average height of *Heterobasidion* spp. of 8.5 meters in Southern Finland. Although the height of *Armillaria* spp. may be shorter, culling of the most significant part of the stem may also occur at final harvest for these fungi (Hylen & Granhus, 2018). In addition, root and butt rot may also lead to reduction in diameter growth. Bendz Hellgren and Stenlid (1995) studied NFI in Sweden and found that the relative diameter growth between healthy and infected trees was increasing over time. Over the period of the last 10 years, the infected trees grew 10.1% slower.

1.4 Previous research and objectives for the thesis

On the subject of rot in spruce in Norway, Granhus and Hylen (2016) and Huse (1983) studied the occurrence of rot on national level. On stand level, Stamnes et al. (2000) studied the rot frequency in older spruce forests, whereas Huse et al. (1994) did a root and butt rot inventory on spruce stumps. In addition, Hylen and Granhus (2018) published a probability model for root and butt rot in individual spruce. Similar to the objective of this thesis, Nilsen (1979) examined the extent of root and butt rots in stems of spruce. Internationally, some studies on the subject of rot height were found in the literary search. Seifert (2007) modelled the rot height by calculating decay cylinders, Honkaniemi et al. (2014) examined the fungal growth in stems with measures from previous studies on the horizontal and vertical spread of the decay, and Bendz Hellgren and Stenlid (1997) examined the extent of decay in relation to tree growth. In addition, Pukkala et al. (2005) examined the height of the decay column dependent on the time since the decay reached the stem base. However, models for practical implementation as for example in in the bucking predictions made by the harvesters has not been developed and assessed in previous studies according to the authors knowledge.

The main objective for this thesis was to develop a practical prediction model for root and butt rot heights in spruce. Furthermore, it was desirable to examine the independent variables that were used in the model and calculate the performance of the model. The practical term of the prediction model is apparent in selection of available variables. The available variables need to be obtainable through stand or single tree characteristics, and to be available before the bucking of a stem into logs begin.

2. MATERIALS AND METHODS

2.1 Study area

The experimental site was located in the south-western part of Innlandet county. More precisely, the stands were located south-east in Etnedal municipality (459 km2). The production forest in Etnedal municipality is spanning over 233,053 da.

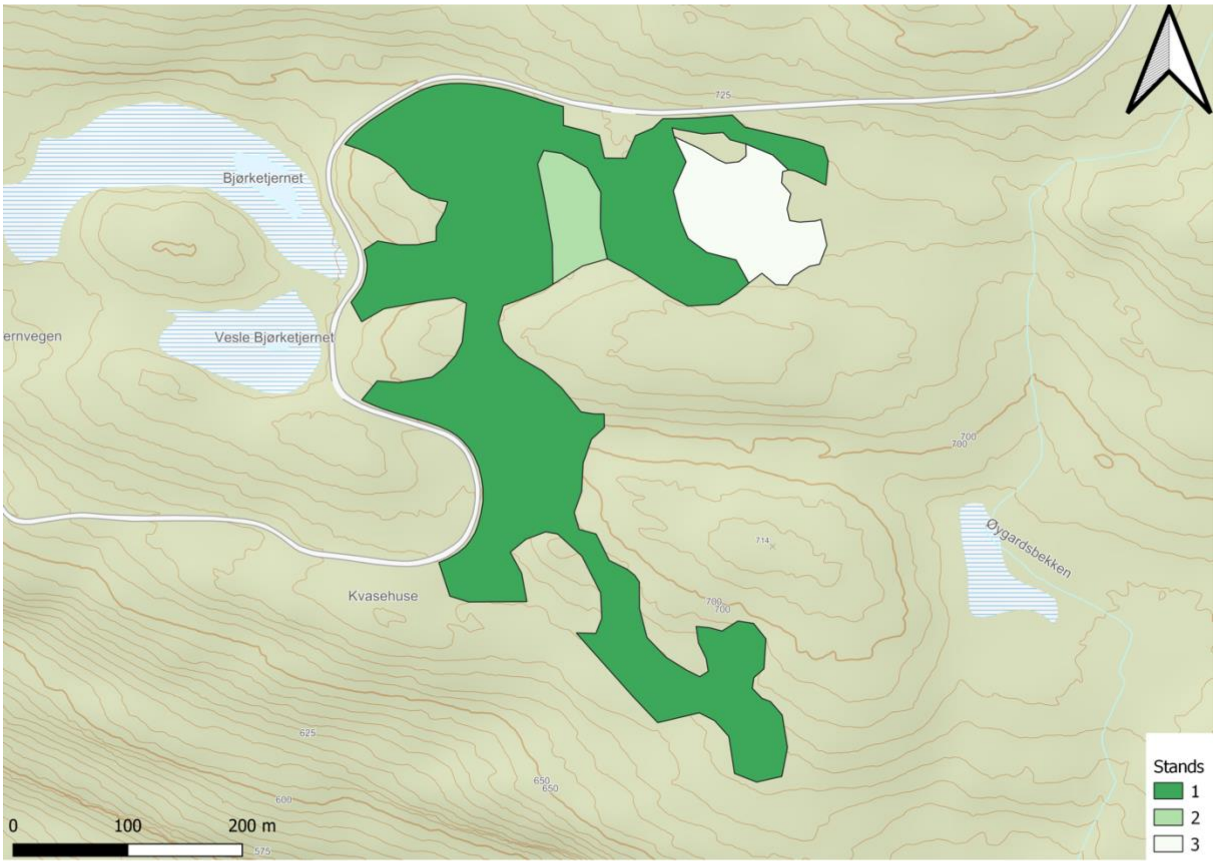

Figure 1. Overview of the study area and respective stands.

The experimental site consisted of three stands totaling 92.3 da (figure 1). The latest forest inventory data was from 2008, however, information on stand 1 was renewed in 2013. Site index for all stands were 11 with spruce as its main tree species. Stand 1 was 131 years old, spanning over 77 da with 95% spruce. Here, the total tree number was 4,258 trees. Stand 2 and 3, respectively, was 4.6 da and 91 years old, and 10.3 da and 81 years old. The total tree number for stand 2 was 179, whereas it for stand 3 was 505. Tree species distributions for stand 2 and 3 were 100% and 90% spruce, respectively. The minor tree species was Scots pine. All three stands were included in the study, however, stand 1 was the main subject of data collection, because it was thought to be the focused for the harvest operation. The western road along stand 1 was built during the stand cycle, whereas trees in the stand were not harvested. The soil structure at the site is categorized as being thin moraine with sandstone as the rock type (Norges Geologiske Undersøkelse, n.d.).

2.2 Field work

The field work and data collection were divided into two missions. The first part consisted of identifying spruce infected with root and butt rot by examining core samples in root-height. The infected trees were clearly marked with colored ribbons, for the purpose of being excluded during the final harvest which occurred about two weeks later. After final harvest, field work part II was initiated. The purpose was to examine the expand of root and butt rot in the preserved spruce which was marked during the first field work, and to examine the root and butt rot extension up the stem. Another thesis was using the same site for sampling (Iversen, 2020). The process and data collection, field work part III, from this thesis will be described in 2.2.3. Data were shared between the studies.

2.2.1 Field work part I

When deciding upon the total number of trees desired in the dataset, it was evident that there would be discrepancies between the number of marked trees and the number of trees available for examination during field work part II. It was suspected that the variation would be caused by damage to the ribbons during final harvest (by trees falling onto ribbon-bearing trees, thereby destroying the marks), insufficient marking of trees making them unobservable by the harvester operator, or marked trees being removed due to the need of roads for the harvester and forwarder during the operational harvest. Thus, for validity, the dataset needed to contain a sufficient number of trees.

It was decided that the sampling would be executed using systematic parallel corridors throughout the stand. For practical reasons the width of the corridors was set to be 2 meters, and a stick of that length was used in the measuring process. The distance between the centerlines in each corridor (a) was adjusted to capture the desired 1,000 trees.

The distance between the centerlines was estimated by:

$$\frac{CW}{\left(\frac{n}{N}\right)} = a$$

Where *CW* is the corridor width, *n* is the total desired number of trees in the sampling process, and *N* is the total number of trees in the stand. *N* was calculated using the latest forest inventory for stand 1 to 4,258 trees. By inserting the relevant values for *CW*, *n*, and *N* we get:

$$\frac{2\ m}{\left(\frac{1000}{4{,}258}\right)} = 8.5\ m$$

If half or more of the tree stem was inside a corridor it was included. All trees in all corridors were drilled with an increment borer under the point of first cut to avoid damaging the logs. The core samples were examined for root and butt rot (figure 2). If a bore sample showed infection, the tree was marked with a colored ribbon.

Figure 2. To the left, the point of the bore samples. To the right, examination and determination of a core sample. Photos: Ole Marius Tollefsen Moen.

The first corridor was placed in the south west corner of the stand. The starting point was set to 4 meters from the stand border which the corridor would follow, in which the stand border was perpendicular to the direction of the corridor. The starting point for each corridor was marked with a bamboo stick, enabling easy positioning of neighboring corridors. While performing the sampling in the corridors, bamboo sticks were used enabling later control and parallel center lines. While performing the sampling, a compass of 400 degrees was used for directional guidance. The bore samples were collected using an electric drill with a custom made device for fitting the 5.15 mm inside of the increment borer to the drill.

Table 1. Number of bore sampled trees and trees that were marked with ribbons during the first field work.

	Day 1	Day 2	Day 3	Day 4	Day 5	Total
Trees sampled	156	120	227	208	98	809
Trees marked	47	32	58	54	24	215

A total of 809 spruce trees were drilled using an increment borer during the first field work. As a result, 215 trees were marked because of detection of rot. Over the course of the five days in the field, the percentages of rot in sampled trees were between 24.5% and 30.1%. The trend shows a decreasing proportion of rot throughout the field work, where the largest percentage was detected during the first day and the smallest the final day. In total, the rot average was 26.6%.

2.2.2 Field work part II

The second field work was carried out with help from a harvester. During the preparation, a sheet for field registration was composed. The registration sheet was constructed to be time-efficient with only necessary variables, due to the cost of hiring the harvester. Furthermore, it was decided to use harvester data in combination with the data collected by Iversen (2020), to reduce time spent in the field. It was essential that all three sources of tree-specific data could be linked to the same tree, therefore, the registration sheet contained a column for tree number, time of first cut and the number of logs with their respective lengths. Firstly, the tree number would the sprayed onto the root, resulting in a link with the data from the other project. Secondly, the time of cut would link the harvester data to the field data. Thirdly, the number of the logs and lengths would determine the expand of root rot. Typically, the position of registration was on the opposite side of the direction of which the tree would be cut.

Furthermore, a visual inspection of the rot was done after that, where the harvester operator moved the stem towards registration position. If the stem showed infection of root and butt rot, cautious bucking was performed to detect the point where the upper side of the log was healthy and the lower side of the log was infected (figure 3). Before the actual data collection started, the harvester operator and I, as the field crew, practiced on a few trees to minimize sources of error and to establish safe working conditions.

In field work part II the trees were harvested in the same order as registered in the first field work. With a desired average precision on the expand of root and butt rot of 25 cm, the last cut on each tree needed to be 50 cm. On trees which were clearly infected, longer cuts were allowed, as long as the last log did not exceed 50 cm.

Figure 3. The work process of the second field work. First, visual inspection of trees (upper left), thereafter bucking with precision to determine the point of rot stop (upper right) and registration of the length of logs and time (lower left). Finally, marking of tree number on the stumps (lower right). The lower right photo also shows the clear-cut area with ribbon marked trees. Photos: Ole Marius Tollefsen Moen.

2.2.3 Field work part III

Data were collected in the same area by Iversen (2020). For the sampling in his thesis, the trees which had been sampled during the field work part II were included. In his sampling, cross-calipered diameter of the stumps and cross-calipered rot diameter was registered. In addition, photographs of stump surfaces were taken. The photographs were used for visual categorization of rot, and would ensure that the desired rot types were included in the dataset.

Table 2. Overview of the visual categorization.

	Number of trees (N)	Percentage (%)
Heterobasidion spp.	16	10.8
Armillaria spp.	40	27.0
Combination	61	41.2
Stem rot [a]	10	6.8
Other [b]	21	14.2
Total	148	100

a Stem rot: rot caused by injuries to the stem and removed from further studies.

b Other: uncertain rot type and removed from further studies.

The classification of rot was later verified by senior research scientist at the Norwegian Institute of Bioeconomy Research (NIBIO), Halvor Solheim. The visual categorization from field work part III (table 2) indicated that the combination of *Heterobasidion* spp. and *Armillaria* spp. was most common in the stand, represented in 41.2% of the cases. Individually, the presence of *Armillaria* spp. was found on 27% of stumps, whereas *Heterobasidion* spp. accounted for 10.8%. The category of “other” was larger than for *Heterobasidion* spp. with a total of 14.2%. The least represented among the categories was stem rot, with a proportion of 6.8%. The root and butt rot fungi in question for this thesis accounts for 79.1% of rot incidences either individually or in combination. On the other side, stem rot and the category of “other” was represented in 20.9% of cases.

2.3 Data processing and validation

Due to the size and context of the bore samples during field work part I, classification of rot was challenging. After the first field work, the total number of spruce with rot (marked spruce) was 215. However, the number reduced to 148 when field work part II was completed. The decline was caused by wrong classification of rot, or due to physical exclusion from final harvest (if a sampled tree was located outside the area of final harvest). Furthermore, there was additional reduction when recording of tree-specific data during field work part III, due to being unable to locate the stumps. This may be caused by damage from the harvester or forwarder, insufficient marking, dirt or the unclear surface in the terrain after final harvest.

At this stage, the harvester tree number and rot heights for rotten energy wood and rotten pulpwood were denoted and linked to the dataset for trees which had harvester information. Based on the HPR file stem profiles, classification of assortments and lengths of logs for each tree were extracted from harvester data and figures describing each tree were made. Furthermore, harvester data contributed with diameter at breast-height, diameter at root and tree height. Measures of the diameter for every 10 cm on the stem up to the final cut were used. The total tree height for each individual tree was calculated using taper functions for spruce (Gjølberg, 1978). Differentiation between assortments of rot was based on the degree of rot on the surface of cut. Assumptions were made for rot assortments, implying that the rot tapered off upwards in the stem from Energy Wood (50% or more decay in the diameter) and ended in Rotten Pulpwood (less than 50% of rot in the diameter of the surface), thereby making Rotten Pulpwood the total rot height. Some trees, per instance double-stemmed trees, had missing values for one of the stems, and were therefore excluded. For the link between manual field registrations and the harvester registrations from field work part II, the time recordings were used in addition to the tree numbering.

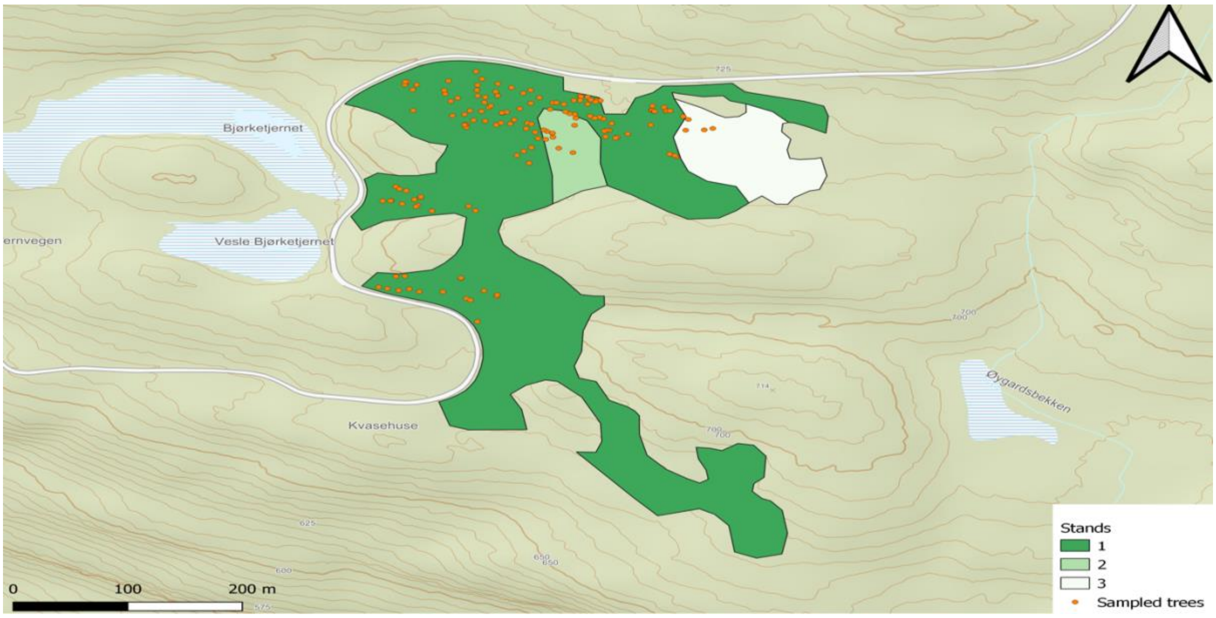

Figure 4. Orange points are positions of trees with rot in the dataset after field work part III.

Finally, dependent upon the visual categorization from field work part III, further processing of the dataset was done by excluding trees without rot. Trees with zero sign of decay, uncertainty of rot type or stem rot was excluded from the dataset. Trees infected with *Heterobasidion* spp., *Armillaria* spp. or a combination of the two were included. Stem rot was detected for some trees along the road in the western part of the area, however, the extension of stem rot within the stand was hard to measure. Based on the last validation, the final dataset contained 117 trees with root and butt rot.

2.4 Statistical methods and data analysis

2.4.1 Rot height prediction models

Prediction models for rot heights was developed using R (R Team, 2019). The dependent variable "rot height" refers to the main prediction model which predicted the total extension of rot in each stem (in other words, the Rotten Pulpwood height). Moreover, the prediction of energy wood was implemented to the main prediction model through a loop.

As mentioned in Kaplan et al. (2014), histograms are compatible in indicating data distributions and its shape, as well as detecting outlier data. Therefore, the examination of variables started visually using the generic built-in function in R for histograms. The dataset was divided into three subsets based on the visual categorization of rot (*Heterobasidion* spp., *Armillaria* spp.

and combination). No significant differentiation between the subsets was found, thus the dataset was handled in entirety. The dependent variable did not show any sign of being normally distributed, and the distribution was right-skewed (positively skewed) in accordance to the description made by Ho and Yu (2015). In fact, the skewness calculated using the e1071-package was 1.06 indicating high skewness (Meyer, 2019). In addressing the skewness for the dependent variable, a log-transformation was performed because it can make skewed data more normally distributed (Feng et al., 2014). Tests for the distribution of the dependent variable, in its original form and as log-transformed, were performed with the descdist-function from the fitdistrplus-package (Delignette-Muller & Dutang, 2019). The descdist-function presents a skewness-kurtosis plot for the empirical distribution of the data, where the distribution is represented visually. Moreover, to account for uncertainty in the estimates of skewness and kurtosis, there is an option for bootstrapping (Delignette-Muller & Dutang, 2019). The dependent variable, in its original form, suggested a Beta-distribution. However, the Beta-distribution follows a distribution from 0 to 1, which is in violation to the values of the dependent variable (Moitra, 1990). Therefore, a trial for the dependent variable where rot height was a percentage of the tree height was performed. The trial did not show any obvious answers to choosing a regression model, and the results from this test was not satisfactory. More secondary tests were conducted, however, the distribution of the dependent variable was not apparent. On the other hand, as regards to the skewness-kurtosis plot, the log-transformed dependent variable could indicate a fit for normal distribution (boot = 1,000). The output data from the regression was analyzed, in addition to the Shapiro-Wilk normality test.

As for the independent variables, the flexibility in selection was reduced due to the model being a practical prediction model. Therefore, the independent variables needed to either be obtained from harvester data before bucking of the stem into logs started or from collectable data throughout the stand. An independent variable for the proportion of rot was used (the rot proportion is calculated by dividing cross-measured diameters of the rot by cross-measured stump diameter from field work part III). It was assumed that this variable could be assessed by operators or by sensors. Another independent variable, tree height, was also included. The total tree height is not available before bucking of the stem. However, as the taper and stem diameters are predicted by measuring diameters in the first part of the stem, total tree height could also be estimated by the harvester computer system. A taper function was also tested as a variable, with the tapering being the average between diameter at root and diameter at breast height. Initially, a linear model with the log-transformed dependent variable was used with the regsubsets-function from the leaps-package. Regsubsets does an extensive search throughout the dataset for the best combination of predictor variables (Lumley, 2020). Moreover, the relationships between potential variables from the regsubsets results were plotted against the dependent variable to examine their relationship, using the ggplot2 package (Wickham, 2005). In ggplot2, the function geom_smooth was used for illustration with linear regression predictions on the relationship between the individual independent variables and the dependent variable before transformation (Prabhakaran, 2016). The linear regression predicted the dependent variable with the data available for each individual independent variable. The predictions were illustrated in graphs for easier visualization. In addition, a variable for tapering of the stems was included in the analysis.

Four multiple linear regression models with the log-transformed dependent variable were developed. The dependent variable *y* with multiple regressors *k* can be described as in Montgomery et al. (2012) at the general form of:

$$\mathcal{Y} = \beta_0 + \beta_1 x_1 + \beta_2 x_2 + \cdots + \beta_k x_k + \mathcal{E}$$ [1]

(1) $\log(rot\ height) = \beta_0 + \beta_1 \times Root\ diameter + \beta_2 \times Rot\ proportion + \mathcal{E}$

(2) $\log(rot\ height) = \beta_0 + \beta_1 \times Root\ diameter + \beta_2 \times Tree\ height + \mathcal{E}$

(3) $\log(rot\ height) = \beta_0 + \beta_1 \times Root\ diameter + \beta_2 \times Rot\ proportion + \beta_3 \times Taper\ function + \mathcal{E}$

(4) $\log(rot\ height) = \beta_0 + \beta_1 \times Root\ diameter + \beta_2 \times Rot\ proportion + \beta_3 \times Tree\ height + \mathcal{E}$

Model selection was based on the estimated coefficients for each model, as well as QQ-plots (quantile-quantile plots) and a Shapiro-Wilk test. The estimated coefficients generated in R were the coefficient estimate, its standard error, t-value and their level of significance. In addition, multiple R-squared and adjusted R-squared were used. Multiple R-squared can be

[1] In Montgomery et al. (2012), β_0 is the value of the dependent variable when all other parameters are set to 0 (the intercept). β_k are estimated coefficients for the independent variables x_k, where changes in x_k has β_k impact on the dependent variable ($\mathcal{Y}$).

described as the amount of variance in the dependent variable that is explained by the independent variables. The adjusted R-squared is an estimate of how the R-squared would be in a population, rather than in the sample. Therefore, it can be used in variable selection because the R-squared will increase when independent variables are included due to correlation, whereas the adjusted R-square will tone this effect down (Miles & Shevlin, 2001). QQ-plots were used with the generic built-in function in R, qqnorm. For the QQ-plots, the residuals of each model were plotted against the normal distribution to examine normality (R Documentation, n.d.-a). The Shapiro-Wilks test has a null-hypothesis that the data come from a normal distribution. Therefore, it was used in evaluating the models (R Documentation, n.d.-b). Finally, on further investigation of the variables, log-transformations of the independent variables "root diameter" and "rot proportion" were performed due to higher scoring parameter estimates. Due to log-transformations, the models needed to be corrected for logarithmic bias before predictions were made. The correction was done by exponentiating and adding half of the mean square error to the intercept-estimate. In addition, as two of the three independent variables were log-transformed, these values were converted back to their original form as described in Flewelling and Pienaar (1981). In the regression, the coefficient estimates were interpreted according to their relationship with the dependent variable, either by log-linear or log-log interpretation (Benoit, 2011; Welham et al., 2014).

As for root and butt rot, *Heterobasidion* spp. and *Armillaria* spp. are the species that was examined and predicted for. For simplicity in calculations, root and butt rot profiles were presumed as having the shape of a cone. Due to differentiation of rot in the assortments (Energy Wood and Rotten Pulpwood), values for predicted height of Energy Wood was also needed for further analysis. A loop was constructed to calculate the value from the prediction model. For the loop, harvester data of every 10 cm of the stem was used. The data contained tree number and stem positions with respective diameters. First, a for-loop exploited the whole dataset. Inside the for-loop, another for-loop was made to run upwards on each stem to the point where an if-test was accepted. Within the inner for-loop, there is a diameter, a rot diameter and a prediction for total rot height. It starts at stem height = 0, and continuous upwards until the proportion of rot is 50%. The rot height for Energy Wood is set to the point of the advancement in the loop, and extracts a value for Energy Wood where more than 50% of the surface is of decay. The result was a table consisting of the total rot height (Rotten Pulpwood) and the height of Energy Wood.

2.4.2 Evaluation of the prediction model in OptApt 2.0.1

To make an optimal bucking of trees into logs OptApt 2.0.1 was used. OptApt is a bucking simulator that produces the most valuable bucking of a stem into logs, using dynamic programming. The pattern of bucking is dependent on quality, dimensions and available prices, thus resulting in the optimal bucking on the available and underlaying information (Gobakken, 2000). OptApt was programmed to perform bucking-to-value. Bucking-to-value is bucking performed solely on price matrices. The optimal solution for cutting a stem is the most valuable among all possible alternatives, for the underlaying price matrices (Kivinen, 2004).

The main objectives for OptApt were to (1) analyze qualities from field registrations and (2) analyze effects of applying the optimal bucking pattern based on predicted rot-heights for rotten pulpwood and rotten energy wood on the field registered quality. The obtained log distributions were compared to distributions based on field registrations. In other words, a comparative study of value on field registered data and data from the prediction model.

To accomplish the objectives, price matrices for spruce assortments were collected and used in OptApt. The following assortments were used: sawn timber, pulpwood, rotten pulpwood, culled rotten pulpwood, energy wood and culled energy wood. The stem profiles and the quality registrations from the harvester data collection were the foundation for tree-specific information. Each individual tree contained records of information for every 10 cm on the stem (as described in 2.3). Furthermore, the positions on the stem had respective information on diameters, denotation for place of bucking, denotation for forced bucking due to discrepancies, and a quality grade. The quality grade is essential in the optimization process and in allocating parts of the stem to correct assortments (table 3). On tree-specific data, quality grade 1 was used for sawn timber, quality 2 was used for rotten pulpwood and quality 4 for energy wood.

Table 3. Overview of assortments (left), minimum and maximum allowed lengths (mid-left), minimum and maximum allowed diameters (mid-right) and necessary quality grade (right). The quality grade of assortments is excluding in hierarchal order, meaning only logs of relevant quality or better is included.

Assortment	Length (cm)	Diameter (mm)	Quality grade
Sawn timber	340 - 586	135 - 530	1
Pulpwood	300 - 550	50 - 700	1
Rotten pulpwood	300 - 530	40 - 550	1 & 2
Rotten pulpwood, culled	5 - 250	40 - 550	1 & 2
Energy wood	300 - 550	50 - 700	1, 2 & 4
Energy wood, culled	5 - 250	40 - 550	1, 2 & 4

The data were used in an optimal bucking-for-value process, where the bucking pattern was extracted for future use (1). Secondly, predicted rot heights from the prediction model were uploaded in OptApt and an optimal bucking-for-value was extracted from this dataset as well (2). Finally, the aforementioned files containing the observed field qualities with the bucking pattern from the predictive data (3) were uploaded and processed. The optimal bucking-for-value on the observed field qualities with the predicted bucking pattern was to resemble the situation a harvester operator would encounter using the developed prediction model as decision support.

3. Results

3.1 The prediction model

The best scoring prediction model (Multiple R-squared and adjusted R-squared were 0.2104 and 0.1894 respectively and a p-value=0.00845 from the Shapiro-Wilk normality test on the residuals) that was used for further examination in this thesis was the model with log-transformed dependent variable and independent variables "root diameter" and "rot proportion". The independent variable "tree height" was not transformed:

$$\log(Rot\ height) = \beta_0 + \beta_1 \times \log(Root\ diameter) + \beta_3 \times Tree\ height + \beta_2 \times \log(Rot\ proportion) + \mathcal{E}$$

Table 4. Coefficient estimates, standard error, t-value and order of significance for the prediction model that was used for this thesis.

Coefficients:	Estimate	Standard Error	t-value	Pr(>t)
Intercept	5.42581	1.36560	3.973	0.000125
log(root diameter)	2.21665	0.57198	3.875	0.000179
Tree height	-0.10739	0.04277	-2.511	0.013457
log(rot proportion)	0.62501	0.15419	4.054	0.000093

As for the coefficient estimates, the tree height estimate was negative. The interpretations of the estimates have to be performed differently (2.4.1). The log-linear interpretation indicates, with all other values unchanged, that a one-unit increase in "tree height" will result in about -10.2% change in "rot height". On the other side, a one-unit decrease in "tree height" will result in about 11.3% change in "rot height". The standard error, however, was relatively small compared to the other coefficients. The independent variables "log(root diameter)" and "log(rot proportion)" was interpreted as a in log-log regression. For a 1% increase in "root diameter", an increase of 2.23% in "rot height" is the result, when all other coefficients are held at the same level. Moreover, a 10% increase in "root diameter" results in an increase of "rot height" of 23.5%. Here, the interpretations for "log(rot proportion)" were that a 1% increase in the independent variable resulted in an increase of 0.62% in “rot height”, with all other coefficients held at the same level. A 10% increase, however, resulted in an increased “rot height” of 6.14%. All coefficients except tree height were significant at p-value=0.001. For “tree height”, the value was larger (p-value=0.01). However, all coefficients were significant at the desired level of p-value=0.05. As for the residuals, the minimum and maximum values were -2.17 and 1.72 m, respectively, and with a median of 0.085 m. With a mean of 0 m, the median is located on the smaller positive side of the mean (see appendix 2, figure 1 for QQ-plots of the residuals and appendix 1, table 1 for estimates on the other models).

The comparison between the predicted rot heights and the field registered rot heights (figure 5, complete list in appendix 1 table 2) showed that the predicted values were more even throughout the dataset. In fact, the minimum value among the predicted was 63.8 cm, whereas it for field registered data was 26 cm. The maximum predicted value was 754.4 cm, here, the maximum field registered rot height was 1,080 cm. The average predicted value was 292.2 cm, with a median of 280.9 cm, whereas respective field registered values were 272.2 cm and 152 cm.

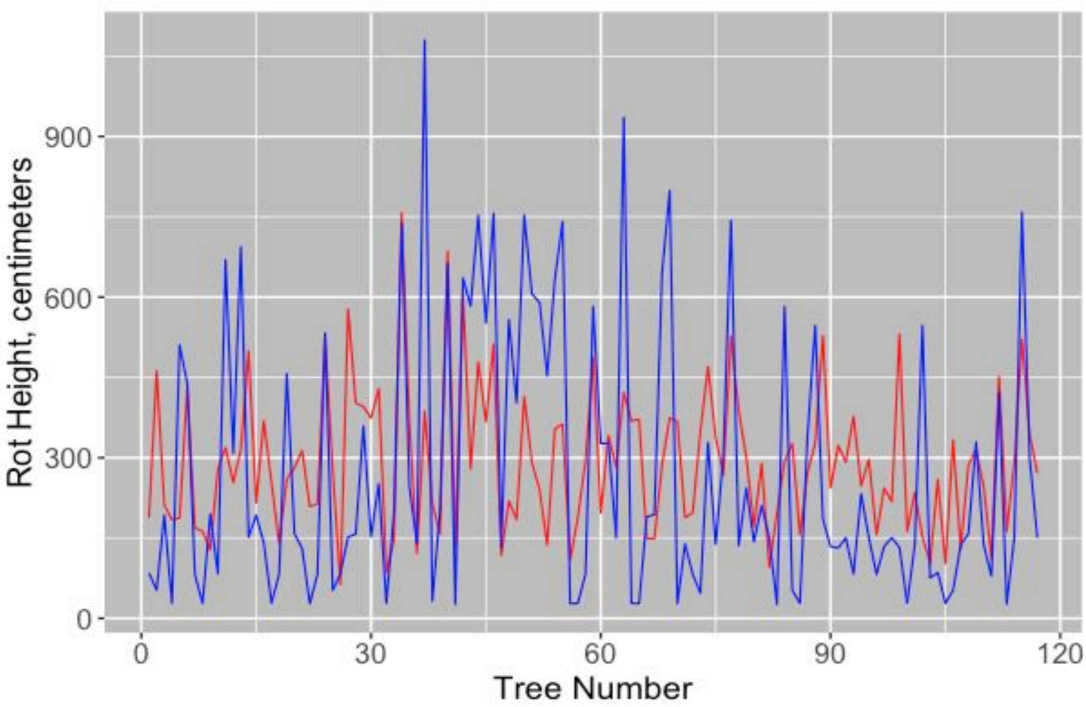

Figure 5. A comparison of rot heights for field registrations (blue line) and predicted rot heights (red line) throughout the dataset of trees. Each individual tree is represented in the graph.

3.1.1 Variables

The transformation of the dependent variable “rot height” is illustrated using a histogram plot (figure 6). For the examination of the relationship between each individual independent variable and the dependent variable, linear regression was used. In the linear regression, the predictive powers of the independent variables on the dependent variable were illustrated (figure 7). The variables are illustrated in their natural form, before log-transformation was performed.

“Root diameter” (figure 7) is increasing over the plot. In general, rot height predictions were higher for higher values of “root diameter”. The confidence interval around the plotted predictions were decreasing to the value around 0.35, where it further increased to settle at a higher level. “Tree height” (figure 7) showed the flattest impact on “rot height”, with starting point on the x-axis of around 2.4 meters and ending at around 4 meters. The respective confidence interval was relatively high. “Rot proportion” (figure 7) showed a positive effect on prediction of rot height. The starting point on the x-axis was about 1.75 meters for the lowest proportions of rot, and ending at the level of 3.75 meters.

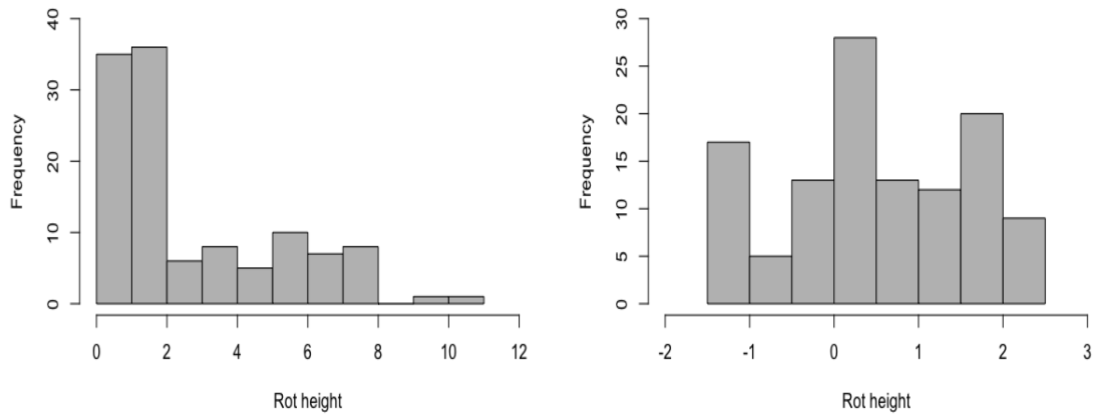

Figure 6. Histogram of the dependent variable before (left) and after log-transformation (right). The dependent variable conformed more to a normal distribution, as implied by the Cullen Frey graph.

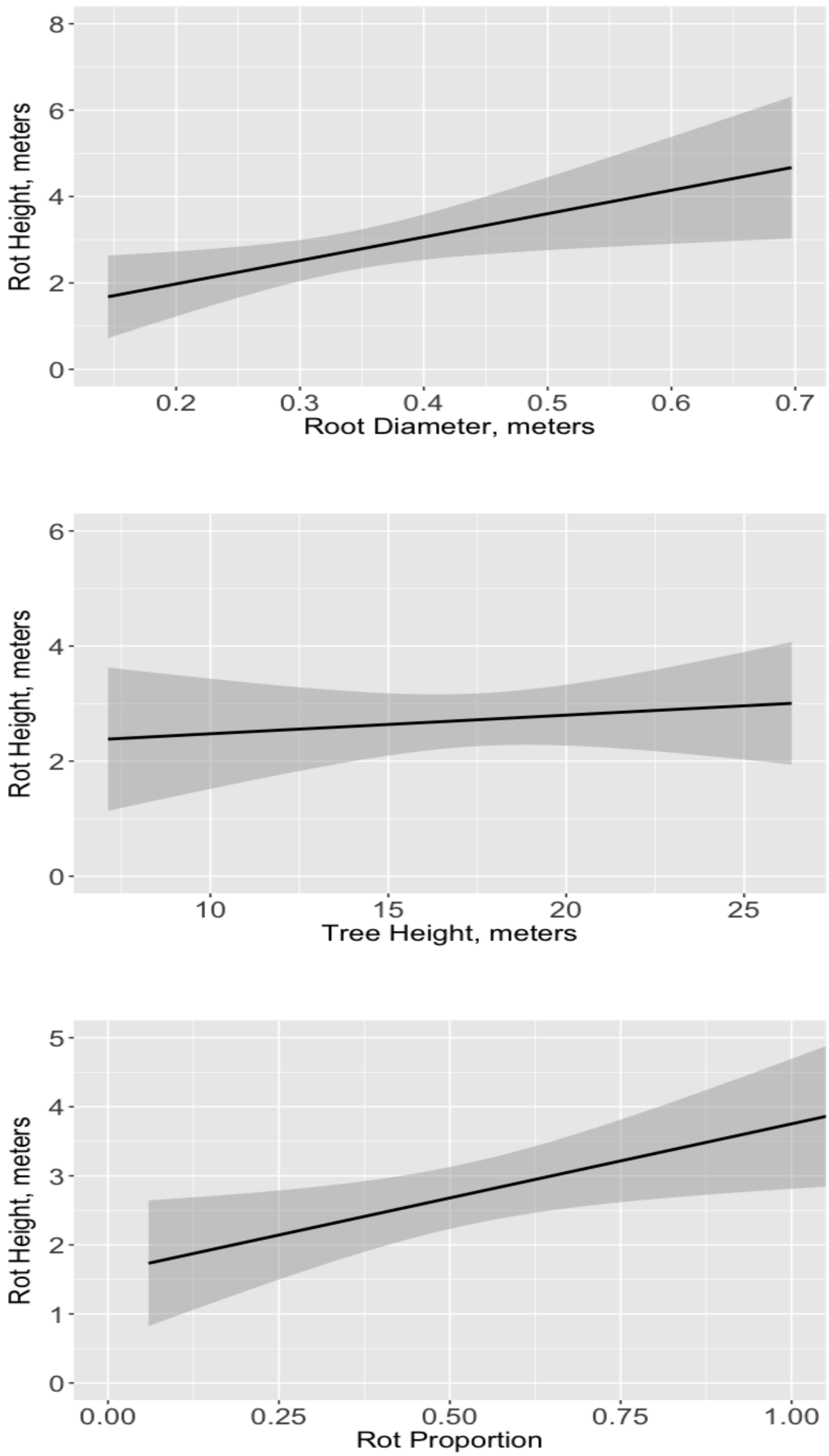

Figure 7. Linear regression with prediction line for the height of rot on the y-axis plotted against independent variables "root diameter" (top), "tree height" (mid) and "rot proportion" (bottom). The shaded area is the 95% confidence interval around the predictions.

3.2 OptApt

In OptApt, a valuation of the optimal bucking based on field registered qualities (table 5, “optimal”) and the optimal bucking pattern from predicted qualities applied on field registered qualities (table 5, “predicted”) were computed. In that way, the results simulated the value of the prediction model and could be compared to the optimal solution.

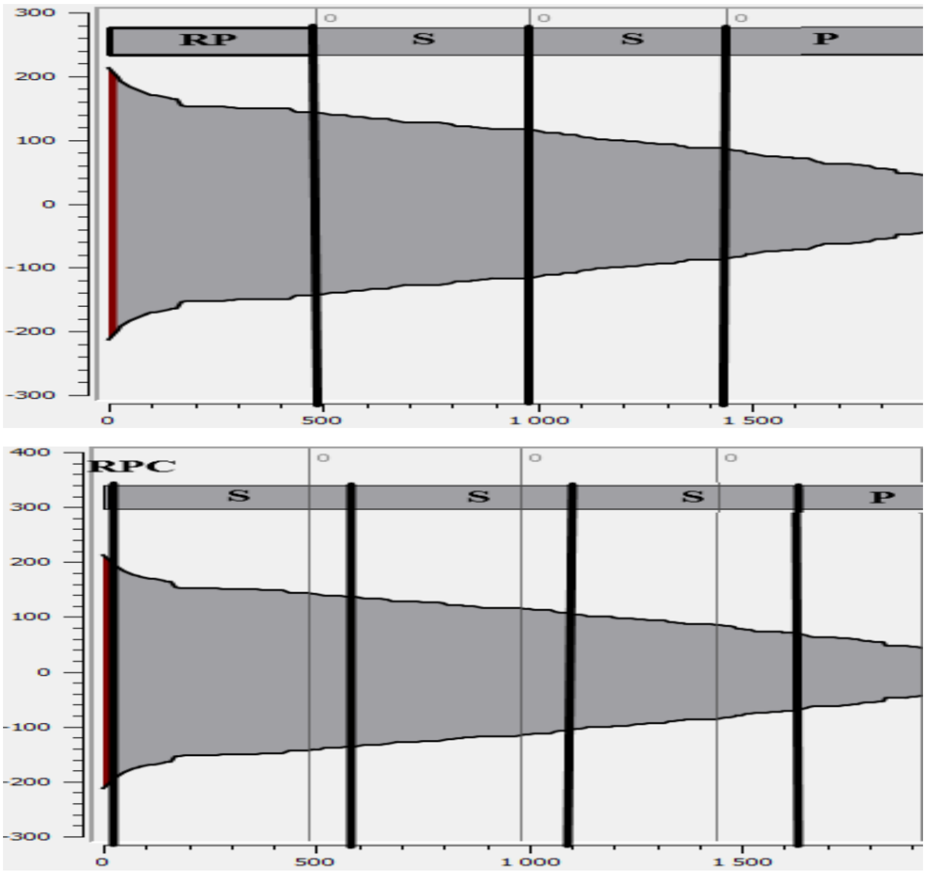

Figure 8. Bucking of example tree no. 41 in the dataset. Predicted bucking on the field observed qualities (top) and optimal bucking of field observed qualities (bottom). RPC=Rotten Pulpwood Culled, RP=Rotten Pulpwood, S=Sawn Timber, P=Pulpwood. Height of the tree (cm) on the x-axis and radius (mm) on the y-axis. The red at the base of the stem is the field registered rot length of 26.5 cm. The predicted rot length is 134.4 cm.

Table 5. Values and volumes for the different assortments when comparing the results of the simulated use of the prediction model and the optimal solution achievable. When added, the volumes for each assortment are less than the total. The differences are due to outlays.

	Predicted		**Optimal**	
Assortment	Value (NOK)	Volume (m^3)	Value (NOK)	Volume (m^3)
Sawn timber	9,759	17.9	16,263	27.5
Pulpwood	3,022	8.4	2,245	6.2
Rotten pulpwood	1,809	5.6	567	1.8
Rotten pulpwood, culled	199	7.1	33	1.2
Energy wood	3,866	12.3	5,440	17.3
Energy wood, culled	21	2.1	10	0.9
Total	18,676	53.7	24,557	55.1

The optimal bucking for the field registered qualities of the trees in the dataset performed NOK 5,881 better than the predicted bucking. Based on the prediction model the average NOK/m^3 was 348. For the optimal solution the value was higher, with NOK/m^3 of 446. The difference in performance was NOK/m^3 98. For the optimal bucking (table 5), larger volumes are classified as sawn timber, thereby creating larger values. The optimal bucking also distinctly allocates higher volumes in Energy wood, whereas the prediction model on average divides more volume in the lesser valuable assortments. In fact, the prediction model showed larger volumes in the assortment for pulpwood than allocated by the optimal bucking procedure. In addition, the total exploited volume was larger for the optimal bucking. For the predicted bucking, the overall value utilization compared to the optimal was 76%. On tree level, this utilization was 74% with a standard error of 18%.

4. Discussion

4.1 Data sampling

Rot inventories on NFI data from the periods 1964-1976 and 1986-2004 indicated a nationwide rot frequency between 7.9%-9.5% (Granhus & Hylen, 2016; Huse, 1983). Nonetheless, in their nationwide study on stump surfaced of spruce, Huse et al. (1994) discovered a root and butt rot proportion of 26.8%. In this particular thesis, it was found that the extent of root and butt rot was 26.6% from increment borer samples, which is in accordance with the latter study. This proportion, approximately 1 out of 4, is also supported by studies in the mid-parts of the country (Næsvold, 1989). However, the sampling technique of using an increment borer in detection of rot has been discussed in previous studies. Stenlid and Wästerlund (1986) found that when sampling at breast height, 80% of all rot was detected and that the percentage increased when sampling at root height. In misjudging of the core samples at stump height, it was emphasized that one reason may be the fact that the decay possesses a lateral expansion, which was harder to detect at that point. This may have led to consequences for this thesis during the sampling of trees, where lateral decay could have been excluded from the dataset. In addition, throughout field work part I, observation of rot in the core samples was acquainted with some degree of doubt due to the small size of the column of wood from the increment borer, as pointed out in Thor et al. (2005). Furthermore, samples may have missed the point of decay, which is likely to have happened for spruce with smaller decay. Therefore, it is possible that the dataset was overrepresented with cases of more advanced decay, and thereby affected the prediction model. Challenges of detecting rot in core samples became evident as the second field work progressed. A smaller number of spruce marked for rot did not show any sign of decay at felling, and on the other side, sampled spruce that was classified as healthy did in fact show decay. Thus, the observed percentage of rot during the first field work is somewhat misguiding and may not be correct, although, these cases were not that common. On another subject, discrimination between fungi, Huse et al. (1994) pointed out that bore samples at breast height leads to underrepresentation of *Armillaria* spp. This may be caused by the fact that the extension of decay up the stem is shorter for this pathogen than for *Heterobasidion* spp. (Solheim, 2010). However, as the samples in this thesis was below the point of first cut, no discrimination between the two species should be present.

The visual categorization during the field work part III (table 2) showed *Armillaria* spp. as the most prominent fungus in that particular stand (27% of all decayed spruce). *Heterobasidion* spp. on the other side, occurred in 10.8% of instances. This is in contrast to previous publications highlighting *Heterobasidion* spp. as the most important root and butt rot fungus in Norway (Hanssen et al., 2019; Stamnes et al., 2000). However, a Norwegian thesis on older spruce on similar altitude conforms with the discovery from the visual categorization, and the importance of *Armillaria* spp. under these conditions (Bjørbæk, 2016). Moreover, the results in this thesis showed that a combination of the two was most common with 41.2% and that the category of "other" was 14.2%. The reason for obscurity in the numbers with large share of combinatory appearances and undefinable rot types can be traced back to the classification itself, where it was stated that a single photograph was not sufficient in cases where the characteristics of the fungi was not distinct. This is also mentioned in Schulze et al. (1997), in addition to the positive side of visual inspection being its effectiveness, whereas the methods of DNA and other molecular analysis is pointed out as time-consuming but accurate. In some cases, lighting and resolution in photographs or dirt on the stumps were hindering factors. In other cases, the decay itself was challenging to interpret. Therefore, the classification was vague and later set aside as it was not a priority for further examination. As the classification was deemed questionable, it is also possible to believe that spruce with unwanted rot types may have been included in the dataset, and on the other side, spruce with the correct rot types may also have been excluded. In addition, smaller decay that was not developed to being distinct could have been left out of the dataset, thereby, inflicting on the prediction model. As the prediction model was made to be of practical functioning, similar root and butt rots to *Heterobasidion* spp. and *Armillaria* spp. may not have added any disturbance if included in the dataset. But, in cases where rot types which differ substantially in characteristics could have been included and might cause errors.

During field work part II, in company with the harvester, some challenges occurred. The challenges were related to handling the small sized logs in regard to the determined precision of 50 cm. In cases where the rot was presumed to extend further up the tree than it actually did, thereby making the first cut above the rot height, the harvester machine operator was able to grab the log, and cut it into smaller logs. The competent operator made the results reliable, as there were uncertain aspects in regard to the execution.

4.2 Data analysis

4.2.1 Sample size

The dataset started out consisting of 215 infected spruce and ended up with a total of 117 (for reasons mentioned in part 2.2.1 and 2.3). The desired amount of 1,000 sampled spruce trees were an optimistic estimate and ended up consisting of 809. In Heckmann et al. (2014), it is mentioned that small sample sizes have consequences for population parameters and regression parameters. The population parameters can obtain large standard errors and wide confidence intervals, in other words, it may have influenced the dependent variable “rot height”. Smaller sample size may also affect the regression parameters, causing the estimates to be uncertain. Moreover, the sample can elude from capturing all variability, thus leaving the model to be insufficient in prediction for different phenomenon. As expected, when the number of observations increases, the associated uncertainty will decrease (Welham et al., 2014). In his study on modelling of rot heights, Seifert (2007) used two different datasets consisting 956 and 863 spruce with the number of stands being 17 and 9 respectively. Although not on the subject of rot, Malinen et al. (2003) predicted the internal quality by using 240 sawn spruce. In his thesis on the extent of root and butt rots in older spruce, Nilsen (1979) examined 130 trees. In this thesis, the reduction in sample size from the original 215 spruce trees after field work part I to the final dataset of 117 was not expected. In general, larger datasets have been used in previous studies. Knofczynski and Mundfrom (2008) states that the sample size for multiple linear regression models are dependent upon objectives of the study and the type of model that is being used. In addition, it is stated that few researchers agree on the minimum sample size. In this thesis, the dependent variable was “rot height”. Root and butt rots (*Heterobasidion* spp. and *Armillaria* spp.) have different characteristics and in respect to the visual categorization, they can also appear different individually. Therefore, when modeling this varying biological phenomenon, a more complete dataset could have captured the variability in its appearance. However, for multiple linear regression models, the Power and Precision in Ryan (2013) suggests a sample size between 36 and 77 for R-squared values between 0.13 and 0.26 (the obtained R-squared in this thesis was 0.21), meaning that the sample size in fact was sufficient to that measure.

4.2.2 Model selection

The dependent variable was left-skewed (figure 6) and did not portray as belonging to any regression model type visually through histograms. The skewness-kurtosis plot of the dependent variable before transformation (appendix 2, figure 2) suggested a Beta-distribution. As the Beta-distribution was abandoned (Materials and methods 2.4.1), the log-transformed dependent variable indicated a fit for linear regression (appendix 2, figure 3). As there was no obvious solution to the distribution of the dependent variable, the suggested multiple linear regression model was chosen. To check assumptions for normality, the output of the regression model was used in evaluation (table 4), in addition to the plotted residuals against the fitted values (appendix 2, figure 4) and the Shapiro-Wilk normality test on the residuals (p-value=0.00845). The Shapiro-Wilk test did not show that the data was normally distributed (p-value<0.05), whereas the somewhat horizontal distribution in the residuals plot could indicate it. However, as stated by Ayinde et al. (2012), the assumptions of the linear regression models are hardly met in real life, and when modeling rot heights, one might think that the uncertainty in the characteristics is a hindering factor. In addition, the assumption of multicollinearity, possible between the independent variables "root diameter" and "rot proportion", could also have been violated. However, in the lack of finding another option, it was deemed as adequate.

4.3 The prediction model

4.3.1 Independent variables

The three independent variables in the model "root diameter", "tree height" and "rot proportion" were assumed as being qualified for a practical prediction model, however, the input data for "tree height" and "rot proportion" would need to come from additional technical gear. The diameter at the root could be extracted at first cut, therefore, the use of this variable was valid. The height of the tree, on the other side, is calculated further up on the stem, and the information on that point in time would be useless for the prediction model. However, the assumption stated that the calculation of tree height could be performed through the predicted taper and stem diameters in the harvester computer system. Another possibility is the combination of single tree based inventory. Here, a combination with airborne laser scanning as in Ene et al. (2012) or by using LIDAR and aerial images as in (Korpela et al., 2007) is a possibility for gathering information on tree heights. The last independent variable is "rot proportion". The current situation is that it is assessed by the harvester operator for determining log quality. For automatic measurement, additional technical gear at the harvester machine would be needed. In their study Ostovar et al. (2019) tested the classification of root and butt rot using computer vision techniques. It is stated that the use of this in operational environments is a relatively new topic.

Individually, the independent variables showed a positive impact on the extent of root and butt rot height (figure 7). "Tree height" made the least impact, however, there was some impact showing that increased height predicted higher values for "rot height". Increase in "root diameter" and "rot proportion" predicted higher levels of "rot height". The result for "rot proportion" is in line with the results in Nilsen (1979) for the relationship between the height of rot and diameter of the rot. The positive relationship between "rot proportion" and the height of rot is also shown in Seifert (2007) for spruce infected with *Heterobasidion* spp., where the proportion of rot is referred to as "relative rot area". Žemaitis and Stakenas (2016) found that increasing stump diameter resulted in significantly larger risk of rot. This is not comparable to the results in this thesis, as they observed rot frequency on stand level, however, the trend may be comparable to the result for "root diameter" as the trees were sampled individually. Mattila and Nuutinen (2007) examined the reduction of sawn-timber volume due to decay of *Heterobasidion* spp., and found that increasing diameter at breast height reduced the sawn-timber percentage. Diameter at breast height is measured above the diameter at root, however, similarities for the measures can be expected. As to the reduction of sawn timber, it can be compared to the extent of the rot as measured in this thesis. Seifert (2007) found a positive relationship between the diameter of the stump on increasing rot height prediction in his two models, for *Heterobasidion* spp. in spruce trees.

The regression estimates for the model (table 4 with accompanying interpretations) showed that "root diameter" had the largest impact on the prediction of "rot height". This is in contrast to the results in Seifert (2007), where his estimate on the proportion of rot were the most influential. However, as the dynamics of the two models is completely different, caution when comparing the two must be taken. In this thesis, the regression estimate "tree height" was negative, whereas it individually showed minimally positive effect on the prediction of "rot height". One reason for the independent variable being negative might be for a reason stated in Tranmer et al. (2020), that the independent variables are fitted together in a linear combination to express the dependent variable. Therefore, as a condition for the assumptions in multiple linear regression, the fitted value becomes negative in combination to the values of the other independent variables.

4.3.2 Prediction model performance

The performance of the prediction model is visualized in table 4 and figure 5. The average predicted root and butt rot height was 292.2 cm, where the average field registered root and butt rot height was 272.2 cm. The two values are relatively close, however, as the medians are 280.9 cm and 152 cm, respectively, the two sources of rot heights differ substantially. For the prediction model, the median indicates that the distributions of values over and under the mean are relatively similar. On the other side, the field registered values indicate that there are more recordings of lower rot heights, making the median substantially lower. In addition, there are some extreme values that is making the mean larger than the median. Visually, this phenomenon is apparent in figure 5, where the predicted values are more even throughout the dataset, and do not cover the variability that was observed during the field work. In addition, this is supported by the minimum and maximum values of 63.8 cm and 754.4 cm for the predictions, whereas the values in the field were 26 cm and 1,080 cm.

The prediction model performance was also evaluated using OptApt. Field registered qualities with the bucking-pattern from the prediction model (the optimal bucking of the predicted rot heights) was compared to the optimal bucking of the field registrations (table 5). Although this is similar to a complete evaluation of the prediction model, some problems occur in the execution. The major difference is that the harvester machine operator, when cutting a tree, will do continuing evaluations of the stem and check for rot. Throughout the process of cutting, the operator will address the situation further and make decisions based on how the root and butt rot is appearing and developing. The model, however, will not be able to address this dynamic and continuing evaluation. It will give predictions for the total extent of rot, and any further evaluation must be performed by the operator. If the bucking of a stem were done according to either the prediction model or the optimal bucking, the result would be as in figure 8. In this example, the prediction model predicts the rot length to be further up the stem than it actually is, thereby creating volume losses with the high first cut. In light of the acquired values for the prediction model and the field registered data, with larger minimum value for the prediction model (63.8 cm) than was registered in the field (26 cm), one might think that for smaller extent of decay around the minimum values, the prediction model would make the cut above the point of rot stop. On the other side, for spruce with larger extent of root and butt rot, it is possible that the cut would be below the actual height of the root and butt rot.

The optimal bucking is based on complete information for the tree stem. In practice, the harvester machine operator will not have that kind of information available. However, reports from Sweden on the utilization grade in a bucking-for-value system show a utilization of approximately 98% for different types of systems (Arlinger & Möller, 2006; Möller et al., 2013). Although this is not completely comparable due to being at different locations under different conditions, the numbers can indicate that it is possible to obtain very high values. As for the utilization for the prediction model it was 76%. At tree level the utilization was 74% with a standard error of 18%. This is significantly smaller than in the aforementioned reports, however, hopefully that the model could have a positive impact on the decisions for harvester operators, as a source for guiding. To truly measure the performance of the model, one would have to cut the stand twice, one time without the model and one time with the model. As this is not possible to do, two near identical stands might have been used. The optimal solution for the stand performed NOK/m^3 98 better than when the prediction model was used, and allocated more volumes to the most valuable of sawn timber (table 5). The reason for this may be that when computing the best bucking of a stem, with all information available, sawn timber is the priority. Therefore, the bucking is executed in a manner that creates the most sawn timber logs. On the other side, the prediction model is basing the quality of the stem on the input at first cut, thereby, further bucking becomes the result of a prediction. Another reason for the better performance can be that when using the prediction model, larger volumes are left in the forest as culled wood. The reason for culling may be that the prediction is wrong, and therefore, the need of culling is present. Whereas the optimal bucking is aware of the qualities, thereby, do not make mistakes on that point.

5. Conclusion

The main objective for this thesis was to develop a practical prediction model for the extent of *Heterobasidion* spp. and *Armillaria* spp. root and butt rot in spruce trees. The results from the model showed that 21.04% of the variance could be explained by the model. Furthermore, the independent variables "root diameter", "tree height" and "rot proportion" were examined for their predictive powers on the dependent variable "rot height". The results from the examination of the independent variables were in accordance to previous publications on the subject. Furthermore, the performance of the model was also evaluated using OptApt, which showed that the prediction model had a utilization grade of 76%. The prediction model in this thesis performed NOK/m^3 98 poorer than the optimal bucking. However, as it is hard to find relevant objects to compare the utilization grade of 76% with, it is concluded that the model can be used for assisting the harvester operator in decision making. In practice, the harvester operator will override predicted bucking when it is discovered that the real quality differs from the predictions.

Addressing the somewhat poor results from the prediction model, the sample size may be emphasized. Other factors may be that root and butt rots are behaving in non-uniform ways, which makes them hard to predict using a multiple linear regression model. However, as this was a practical prediction model, the number of available independent variables when predicting rot height was constrained.

In future research, similar prediction models should be developed using a larger number of observations and implemented in the computer system in the harvesters to evaluate how much the predictions could help guiding the bucking. That improvement in bucking decisions is the payoff of further developing the model.

6. References

Allikmäe, E., Laarmann, D. & Korjus, H. (2017). Vitality Assessment of Visually Healthy Trees in Estonia. *Forests 2017*, 8 (7): 1-8. doi: 10.3390/f8070223.

Arlinger, J. & Möller, J. J. (2006). *Virkesvärdestest 2006 – skördardatorer*. Rapport från Skogforsk nr. 6 2007. Available at: https://www.skogforsk.se/cd_20190114161755/contentassets/c387d988998048efaf044a008cb84573/resultat6-07-lowres.pdf (accessed: 20.05.2020).

Asiegbu, F. O., Adomas, A. & Stenlid, J. (2005). Conifer root and butt rot caused by *Heterobasidion annosum* (Fr.) Bref. s.l. *Molecular Plant Pathology*, 6: 395-409. doi: 10.1111/j.1364-3703.2005.00295.x.

Axmon, J., Hansson, M. & Sörnmo, L. (2004). Experimental study on the possibility of detecting internal decay in standing *Picea abies* by blind impact response analysis. *Forestry: An International Journal of Forest Research*, 77 (3): 179-192. doi: 10.1093/forestry/77.3.179.

Ayinde, K., Apata, E. O. & Alaba, O. O. (2012). Estimators of Linear Regression Model and Prediction under Some Assumption Violation. *Open Journal of Statistics*, 2 (5): 534-546. doi: 10.4236/ojs.2012.25069.

Bendz Hellgren, M. & Stenlid, J. (1995). Long-term reduction in the diameter growth of butt rot affected Norway spruce, *Picea abies*. *Forest Ecology and Management*, 74 (1-3): 239-243. doi: 10.1016/0378-1127(95)03530-N.

Bendz Hellgren, M. & Stenlid, J. (1997). Decreased volume growth of *Picea abies* in response to *Heterobasidion annosum* infection. *Canadian Journal Forest Resources*, 27: 1519-1524. doi: 10.1139/x97-104.

Benoit, K. (2011). *Linear Regression Models with Logarithmic Transformations*. Available at: https://kenbenoit.net/assets/courses/ME104/logmodels2.pdf (accessed: 01.05.2020).

Bjørbæk, L. H. (2016). *Råte i høyereliggende granskog på Østlandet*. Master´s Thesis. Ås: Norwegian University of Life Sciences. Available at: https://nmbu.brage.unit.no/nmbu-xmlui/handle/11250/2403128 (accessed: 15.04.2020).

Bøhmer, E. & Aarnes, H. (2017). tre - plante. In *Store norske leksikon*. Available at: https://snl.no/tre_-_plante (accessed: 26.03.2020).

Cadullo, G., Tinner, W. & Rigo, D. d. (2016). *Picea abies* in Europe: distribution, habitat, usage and threats. In *European Atlas of Forest Tree Species*. Available at: https://ies-ows.jrc.ec.europa.eu/efdac/download/Atlas/pdf/Picea_abies.pdf (accessed: 26.03.2020).

Delignette-Muller, M.-L. & Dutang, C. (2019). *descdist: Description of an empirical distribution for non-censored and cencored data*. Available at: https://rdrr.io/cran/fitdistrplus/man/descdist.html (accessed: 01.04.2020).

Ene, L., Næsset, E. & Gobakken, T. (2012). Single tree detection in heterogeneous boreal forests using airborne laser scanning and area-based stem number estimates.

International Journal of Remote Sensing, 33 (16): 5171-5193. doi: 10.1080/01431161.2012.657363.

Feng, C., Wang, H., Lu, N., Chen, T., He, H., Lu, Y. & Tu, X. M. (2014). Log-transformation and its implications for data analysis. *Shanghai Archive of Psychiatry*, 26 (2): 105-109. doi: 10.3969/j.issn.1002-0829.2014.02.009.

Flewelling, J. W. & Pienaar, L. V. (1981). Multiplicative Regression with Lognormal Errors. *Forest Science*, 27 (2): 281-289. doi: 10.1093/forestscience/27.2.281.

Garbelotto, M. & Gonthier, P. (2013). Biology, Epidemiology, and control of *Heterobasidion* Species Worldwide. *Annual Review of Phytopathology*, 51: 39-59. doi: 10.1146/annurev-phyto-082712-102225.

Gellerstedt, S. (2002). Operation of the Single-Grip Harvester: Motor-Sensory and Cognitive Work. *International Journal of Forest Engineering*, 13 (2): 35-47. doi: 10.1080/14942119.2002.10702461.

Giordano, L., Sillio, F., Guglielmo, F. & Gonthier, P. (2015). Comparing visual inspection of trees and molecular analysis of internal wood tissues for the diagnosis of wood decay fungi. *An International Journal of Forest Research*, 88 (4): 465-470. doi: 10.1093/forestry/cpv015.

Gjølberg, R. (1978). Et EDB-program for analyse av verdiutviklingen for enkelttrær ved råteangrep. *Department of Forest Economics*, 2: 48.

Gobakken, T. (2000). The effect of two different price systems on the value and cross-cutting patterns of Norway spruce logs. *Scandinavian Journal of Forest Research*, 15 (3): 368-377. doi: 10.1080/028275800448002.

Granhus, A. & Hylen, G. (2016). *Råte i granskog - utbredelse og konsekvenser for valg av omløpstid*. NIBIO Rapport 2/40. Available at: https://nibio.brage.unit.no/nibio-xmlui/bitstream/handle/11250/2380089/NIBIO_RAPPORT_2016_2_40.pdf?sequence=3&isAllowed=y (accessed: 26.03.2020).

Hanssen, K. H., Solberg, S., Hietala, A., Krokene, P., Rolstad, J., Solheim, H. & Økland, B. (2019). *Skogskader - en kunnskapssammenstilling*. NIBIO Rapport 5/143. Available at: https://nibio.brage.unit.no/nibio-xmlui/handle/11250/2632291 (accessed: 26.03.2020).

Heckmann, T., Gegg, A. & Becht, M. (2014). Sample size matters: investigating the effect of sample size on a logistic regression susceptibility model for debris flows. *Natural Hazards and Earth System Sciences*, 14: 259-278. doi: 10.5194/nhess-14-259-2014.

Ho, A. D. & Yu, C. C. (2015). Descriptive Statistics for Modern Test Score Distributions: Skewness, Kurtosis, Discreteness, and Ceiling Effects. *Educational and Psychological Measurement*, 75 (3): 365-388. doi: 10.1177/0013164414548576.

Honkaniemi, J., Ojansuu, R., Piri, T., Kasanen, R., Lehtonen, M., Salminen, H., Kalliokoski, T. & Mäkinen, H. (2014). Hmodel, a *Heterobasidion annosum* model for even-aged Norway spruce stands. *Canadian Journal Forest Resources*, 44 (7): 796-809. doi: 10.1139/cjfr-2014-0011.

Huse, K. J. (1983). *Forekomst av råte i norsk granskog* Rapport fra Norsk institutt for skogforskning 3/1 : 1-39 (accessed: 26.03.2020).

Huse, K. J., Solheim, H. & Venn, K. (1994). *Råte i gran registrert på stubber etter hogst vinteren 1992*. Research paper of Skogforsk 23/94. Available at:

https://nibio.brage.unit.no/nibio-xmlui/bitstream/handle/11250/2560332/Skogforsk-Rapport-1994-23.pdf?sequence=1&isAllowed=y.

Hylen, G. & Granhus, A. (2018). A probability model for root and butt rot in *Picea abies* derived from Norwegian national forest inventory data. *Scandinavian Journal of Forest Research*, 33 (7): 657-667. doi: 10.1080/02827581.2018.1487074.

Iversen, E. A. (2020). *Detection of root and butt rot in Norway Spruce (Picea Abies) using airborne hypersepctral images and laser scanner - in submission*. Master´s thesis. In Submission: Norwegian University of Life Sciences.

Kaplan, J. J., Gabrosek, J. G., Curtiss, P. & Malone, C. (2014). Investigating Student Understanding of Histograms. *Journal of Statistics Education*, 22 (2): 1-30. doi: 10.1080/10691898.2014.11889701.

Keča, N. & Solheim, H. (2011). Ecology and distribution of *Armillaria* speies in Norway. *Forest Pathology*, 41 (2): 120-132. doi: 10.1111/j.1439-0329.2010.00644.x.

Kivinen, V.-P. (2004). A Genetic Algorithm Approach to Tree Bucking Optimization. *Forest Science*, 50 (5): 696-710. doi: 10.1093/forestscience/50.5.696.

Knofczynski, G. T. & Mundfrom, D. (2008). Sample Sizes when Using Multiple Linear Regression for Prediction. *Educational and Psychological Measurement*, 68 (3): 431-442. doi: 10.1177/0013164407310131.

Korpela, I., Dahlin, B., Schafer, H., Bruun, E., Haapaniemi, F., Honkasalo, J., Ilvesniemi, S., Kuutti, V., Linkosalmi, M., Mustonen, J., et al. (2007). Single-tree forest inventory using lidar and aerial images for 3D treetop positioning, species recognition, height and crown width esimation. *Laser Scanning 2007 and SilviLaser 2007*: 1-8. doi: N/A : https://www.isprs.org/proceedings/xxxvi/3-w52/final_papers/Korpela_2007.pdf.

Lumley, T. (2020). *Regression Subset Selection*. Available at: https://cran.r-project.org/web/packages/leaps/leaps.pdf (accessed: 02.04.2020).

Malinen, J., Matamo, M. & Verkasalo, E. (2003). Predicting the internal quality and value of Norway spruce trees by using two non-parametric nearest neighbor methods. *Forest Products Journal*, 53 (4): 85-94. doi: N/A: https://jukuri.luke.fi/handle/10024/510586.

Mattila, U. & Nuutinen, T. (2007). Assessing the Incidence of Butt Rot in Norway Spruce in Southern Finland. *Silva Fennica*, 41 (1): 29-43. doi: 10.14214/sf.473.

Mester, T., Varela, E. & Tien, M. (2004). Wood Degredation by Brown-Rot and White-Rot Fungi. *Genetics and Biotechnology. The Mycota (A Comprehensive Treatise on Fungi as Experimental Systems for Basic and Applied Research)*, 2: 355-368. doi: 10.1007/978-3-662-07426-8_17.

Meyer, D. (2019). *e1071: Misc Functions of the Department of Statistics, Probability Theory Group (Formerly: E1071)*. Available at: https://cran.r-project.org/web/packages/e1071/index.html (accessed: 01.04.2020).

Miles, J. & Shevlin, M. (2001). *Applying Regression and Correlation: A Guide for Students and Researchers*. 1 ed.: SAGE Publications Ltd., London, Thousand Oaks.

Ministry of Agriculture and Food. (2015). *SKOG22*. Nasjonal strategi for skog- og trenæringen. Available at: https://www.regjeringen.no/contentassets/711e4ed8c10b4f38a699c7e6fdae5f43/skog_22_rapport_260115.pdf?fbclid=IwAR3fmzkgUCdyciNexkyhiCQqEj9m12Lkn5kqyAmbmkbEApVrMMgxZ7nCP84 (accessed: 26.03.2020).

Moitra, S. D. (1990). Skewness and the Beta Distribution. *The Journal of the Operational Research Society*, 41 (10): 953-961. doi: 10.2307/2583273.

Möller, J. J., Arlinger, J. & Nordström, M. (2013). *Test av StandForD 2010 - Implementation and test of harvester*. Arbetsrapport från Skogforsk 798-2013. Available at: https://www.skogforsk.se/cd_20190114161833/contentassets/3bb2cbc73b254e18b7475fa23bb16236/test-av-stanford-2010-implementation-i-skordare-stanford-2010-implementation-and-test-of-harvester.pdf (accessed: 20.05.2020).

Montgomery, D. C., Peck, E. A. & Vining, G. G. (2012). *Introduction to Linear Regression Analysis*. 5 ed.: John Wiley & Sons, Inc., Hoboken, New Jersey.

Næsvold, B. H. (1989). *Forekomst av råte i eldre granskog: en undersøkelse under hogst og på hogstflatene i Nord-Trøndelag*. Steinkjer: NFT.

Nilsen, P. (1979). *Variasjon i rotråtens utbredelse i stammen hos eldre gran i forhold til egenskaper hos det enkelte treet*. Master´s thesis. Ås: Norges Landbrukshøgskole (NLH).

Norges Geologiske Undersøkelse. (n.d.). *Nasjonal Arealinformasjon - Berggrunnskart*: NGU. Available at: http://geo.ngu.no/kart/arealis/?fbclid=IwAR3Vh_x3K6Wrxqyq_z7oCnNRvQglvDvEa8Cq-wdPPsLCkTMc_qlWq1KOsvs (accessed: 10.04.2020).

Norsk Virkesmåling. (2015a). *Målereglement Massevirke*. Available at: http://www.m3n.no/wp-content/uploads/2017/09/B2_Maalereglement_massevirke.pdf (accessed: 06.04.2020).

Norsk Virkesmåling. (2015b). *Målereglement Sagtømmer*. Available at: http://www.m3n.no/wp-content/uploads/2017/09/B1_Maalereglement_sagtommer.pdf (accessed: 06.04.2020).

Norsk Virkesmåling. (n.d.-a). Available at: http://www.m3n.no/ (accessed: 06.04.2020).

Norsk Virkesmåling. (n.d.-b). *Målemetoder*. Available at: http://www.m3n.no/tjenester/malemetoder/.

Ostovar, A., Talbot, B., Puliti, S., Astrup, R. & Ringdahl, O. (2019). Detection and Classification of Root and Butt-Rot (RBR) in Stumps of Norway Spruce Using RGB Images and Machine Learning. *Sensors*, 19 (7): 1-14. doi: 10.3390/s19071579.

Øvrum, A. & Vestøl, G. I. (2009). Modeling the effect of length on yield of sawn timber grades in Norway spruce (*Picea abies*(L.) Karst.). *European Journal of Wood and Wood Products*, 67: 63–70. doi: 10.1007/s00107-008-0286-9.

Prabhakaran, S. (2016). *R-statistics: Loess - Local Regression*. Available at: http://r-statistics.co/Loess-Regression-With-R.html (accessed: 15.04.2020).

Pukkala, T., Möykkynen, T., Thor, M., Rönnberg, J. & Stenlid, J. (2005). Modeling infection and spread of *Heterobasidion annosum* in even-aged Fennoscandian conifer stands. *Canadian Journal Forest Resources*, 35 (1): 74-84. doi: 10.1139/x04-150.

R Documentation. (n.d.-a). *Quantile-Quantile Plots*. Available at: https://stat.ethz.ch/R-manual/R-devel/library/stats/html/qqnorm.html (accessed: 04.04.2020).

R Documentation. (n.d.-b). *Shapiro-Wilk Normality Test*. Available at: https://www.rdocumentation.org/packages/stats/versions/3.6.2/topics/shapiro.test (accessed: 04.04.2020).

R Team. (2019). *RStudio: Integrated Development Environment for R*. Available at: https://rstudio.com/about/ (accessed: 01.04.2020).

Risbeth, J. (1985). Infection cycle of *Armillaria* and host response. *European Journal of forest Pathology*, 15: 332-341. doi: 10.1111/j.1439-0329.1985.tb01108.x.

Ryan, T. P. (2013). *Sample Size Determination and Power*: John Wiley & Sons Inc., Hoboken, New Jersey.

Ryvarden, L. (2019). Råte. In *Store norske leksikon*. Available at: https://snl.no/r%C3%A5te (accessed: 30.03.2020).

Schulze, S., Bahnweg, G., Tesche, M. & Sandermann Jr, H. (1997). Identification techniques for *Armillaria* spp. and *Heterobasidion annosum* root and butt rot diseases. *Archives of Phytopathology & Plant Protection*, 31 (2): 141-163. doi: 10.1080/03235409709383225

Seifert, T. (2007). Simulating the extent of decay caused by *Heterobasidion annosum* s. l. in stems of Norway spruce. *Forest Ecology and Management*, 248 (1-2): 95-106. doi: 10.1016/j.foreco.2007.02.036.

Skogbrukslova. (2005). *Lov om skogbruk av 27.05.2005 nr 8*. Available at: https://lovdata.no/dokument/NL/lov/2005-05-27-31?q=m%C3%A5ling%20skogsvirke (accessed: 06.04.2020).

Solheim, H. (2010). *Råte i levende trær*. Ås: Norwegian Forest and Landscape Institute. Available at: https://nibio.brage.unit.no/nibio-xmlui/bitstream/handle/11250/2469366/SoL-Brosjyre-2010-R%25C3%25A5tesopper%2Bi%2Blevende%2Btr%25C3%25A6r.pdf?sequence=1&isAllowed=y (accessed: 27.03.2020).

Stamnes, V. S. G., Solberg, S. & Solheim, H. (2000). An analysis of the frequency of rot in old spruce forest, and from forest, climatic and edaphic factors. *Rapport fra Skogforskningen* (No. 17): 16 pp. doi: N/A.

Statistisk Sentralbyrå. (2019). *Fakta om skogbruk*. Available at: https://www.ssb.no/jord-skog-jakt-og-fiskeri/faktaside/skogbruk (accessed: 25.03.2020).

Statistisk Sentralbyrå. (2020). *Skogavvirkning for salg*. Available at: https://www.ssb.no/skogav (accessed: 25.03.2020).

Stenlid, J. & Wästerlund, I. (1986). Estimating the frequency of stem rot in *Picea abies* using an increment borer. *Scandinavian Journal of Forest Research*, 1 (1-4): 303-308. doi: 10.1080/02827588609382421.

Stenlid, J. & Redfern, D. B. (1998). Spread within the tree and stand: *Heterobasidion annosum*. 125-141.

Tamminen, P. (1985). *Butt rot in Norway spruce in southern Finland*. Communicationes Instituti Forestalis Fenniae. Available at: https://jukuri.luke.fi/handle/10024/522535 (accessed: 10.04.2020).

Thor, M., Ståhl, G. & Stenlid, J. (2005). Modelling root rot incidence in Sweden using tree, site and stand variables. *Scandinavian Journal of Forest Research*, 20 (5): 165-176. doi: 10.1080/02827580510008347.

Tomter, S. M. & Dalen, L. S. (2018). *Skogens klimagassregnskap*. Bærekraftig skogbruk i Norge. Available at: http://www.skogbruk.nibio.no/klimagassregnskapet-for-norske-skoger (accessed: 26.03.2020).

Tranmer, M., Murphy, J., Elliot, M. & Pampaka, M. (2020). *Multiple Lnear Regression (2nd Edition)*. Cathie Marsh Institute Working Paper 2020-01. Available at: http://hummedia.manchester.ac.uk/institutes/cmist/archive-publications/working-papers/2020/multiple-linear-regression.pdf (accessed: 10.05.2020).

Vollbrecht, G. & Agestam, E. (1995). Identifying butt rotted Norway spruce trees from external signs. *Forest and Landscape Research*, 1 (3): 241-254. doi: N/A.

Welham, S. J., Gezan, S. A., Clark, S. J. & Mead, A. (2014). *Statistical Methods in Biology: Design and Analysis of Experiments and Regression*: CRC Press, Taylor & Francis Group, Boca Ranton, FL.

Wickham, H. (2005). *ggplot2*. Available at: https://ggplot2.tidyverse.org/ (accessed: 10.04.2020).

Žemaitis, P. & Stakenas, V. (2016). Ecological factors influencing frequency of Norway spruce butt rot in mature stands in Lithuania. *Russian Jounal of Ecology*, 47: 355-363. doi: 10.1134/S1067413616040172.

Appendix 1 – Tables

Appendix, table 1. Coefficient estimates, multiple R-squared, adjusted R-squared and Shapiro-Wilk test for all models in this thesis. The highlighted values are the best scoring. Model 4 was further developed and used in the thesis.

	Multiple R-squared	Adjusted R-squared	Shapiro-Wilk Test
Model 1	0.1231	0.1077	0.003833
Model 2	0.08724	0.07123	0.001442
Model 3	0.1315	0.1085	**0.006203**
Model 4	**0.1541**	**0.1317**	0.002649

Appendix, table 2. List of tree number with values for: predicted energy wood, predicted rotten pulpwood, field registered energy wood and field registered rotten pulpwood, respectively.

Tree number	Predicted Energy Wood	Predicted Rotten Pulpwood	Energy Wood, field	Rotten Pulpwood, field
1	0	188.2	0	84.5
2	0	462.6	0	52.5
3	0	212.1	0	193
4	0	184.1	0	28
5	0	187.5	0	510.5
6	200	428.6	152.5	439
7	0	169.0	0	82
8	0	162.5	0	27.5
9	0	127.6	0	195
10	0	278.7	0	83
11	0	319.0	0	670
12	70	253.7	308	308
13	200	315.1	457.5	694
14	260	499.6	151.5	151.5
15	0	215.9	0	192.5
16	0	369.5	0	140.5
17	0	252.6	0	28
18	0	139.5	0	83
19	120	260.7	0	457
20	0	280.9	0	158
21	80	313.7	0	130.5
22	0	208.8	0	27.5
23	0	213.9	0	82
24	290	523.9	150.5	533
25	120	275.5	0	52
26	0	63.1	0	84
27	320	577.4	152	152
28	180	402.4	157.5	157.5
29	190	395.3	359	359
30	200	374.1	152	152

31	0	429.2	0	251.5
32	0	86.0	0	28
33	0	146.2	0	199.5
34	400	757.4	150.5	738
35	60	366.3	0	246
36	0	121.1	0	139
37	200	386.8	455.5	1080
38	60	215.0	0	32
39	50	158.1	0	199
40	390	685.5	152.5	663.5
41	0	134.4	0	26.5
42	380	608.3	455	635.5
43	100	279.1	164.5	583
44	280	478.8	753	753
45	180	366.5	151.5	551.5
46	290	512.2	756	756
47	0	117.7	0	132.5
48	0	219.0	0	558
49	40	184.4	402	402
50	180	414.3	753	753
51	150	290.8	152	606
52	130	240.9	151	590
53	40	136.5	452.5	452.5
54	180	353.6	150.5	633.5
55	180	362.8	452.5	741
56	0	108.3	0	27.5
57	0	188.1	0	28
58	150	294.2	0	82.5
59	210	487.0	150.5	582.5
60	120	196.7	150.5	326.5

61	0	341.3	150.5	327.5
62	130	282.1	150.5	150.5
63	0	422.2	758	935.5
64	260	368.5	0	28
65	0	371.6	0	28
66	0	148.9	0	189.5
67	0	149.1	0	194
68	0	287.3	150.5	645
69	230	374.5	451.5	798.5
70	210	367.9	0	27
71	0	188.4	0	139
72	0	196.7	0	82.5
73	0	349.2	0	47
74	300	470.2	151	328.5
75	230	337.7	0	138
76	0	267.2	0	304
77	250	527.5	452.5	743.5
78	150	388.3	0	136
79	200	301.0	0	243.5
80	30	170.8	0	143
81	100	289.5	0	211
82	50	95.2	150.5	150.5
83	0	196.4	0	26
84	0	293.1	150.5	582.5
85	250	327.0	0	52.5
86	0	156.2	0	28
87	0	272.6	0	343
88	0	327.5	155.5	547
89	250	528.1	0	186
90	100	243.5	0	134

91	0	322.5	0	131.5
92	180	291.6	150.5	150.5
93	0	377.8	0	83
94	0	247.5	0	232.5
95	140	296.8	151	151
96	0	156.4	0	82
97	140	243.3	0	134.5
98	110	217.9	150.5	150.5
99	270	530.9	0	132.5
100	40	161.9	0	28
101	0	235.0	0	137
102	0	152.7	0	547
103	0	102.8	0	75.5
104	50	259.5	0	85.5
105	0	102.4	0	28
106	170	333.2	0	52.5
107	0	130.4	0	137.5
108	0	285.8	0	157.5
109	150	316.0	150.5	329
110	0	246.4	0	138
111	0	112.8	0	79
112	220	451.8	0	421.5
113	0	162.6	0	26.5
114	20	291.8	151.5	151.5
115	300	521.0	453	759
116	150	344.4	0	298.5
117	140	271.2	150.5	150.5

Appendix 2 – Figures

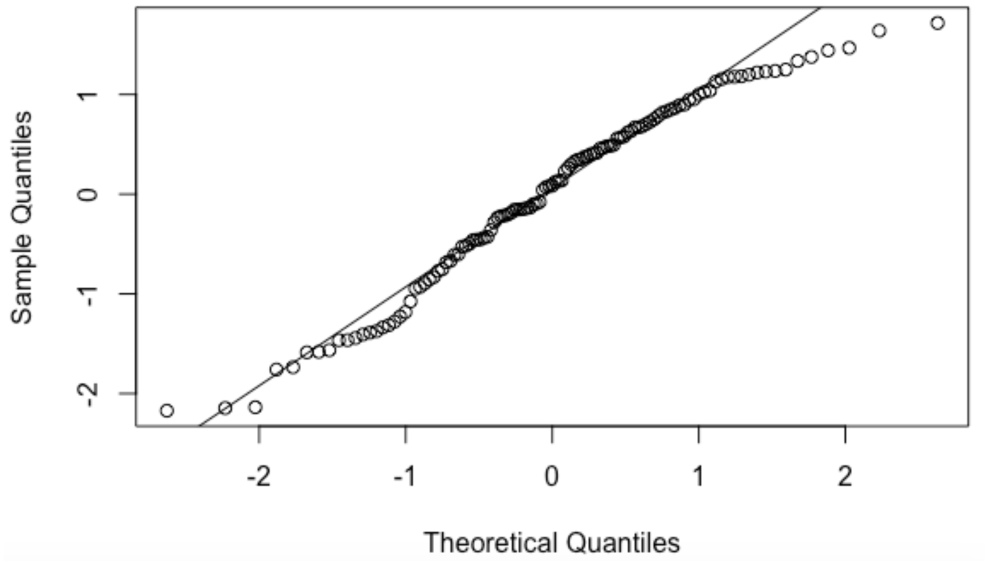

Appendix, figure 1. Quantile-Quantile plot of the sample quantiles against the theoretical straight quantiles. The sample quantiles are derailing from the line in some degree.

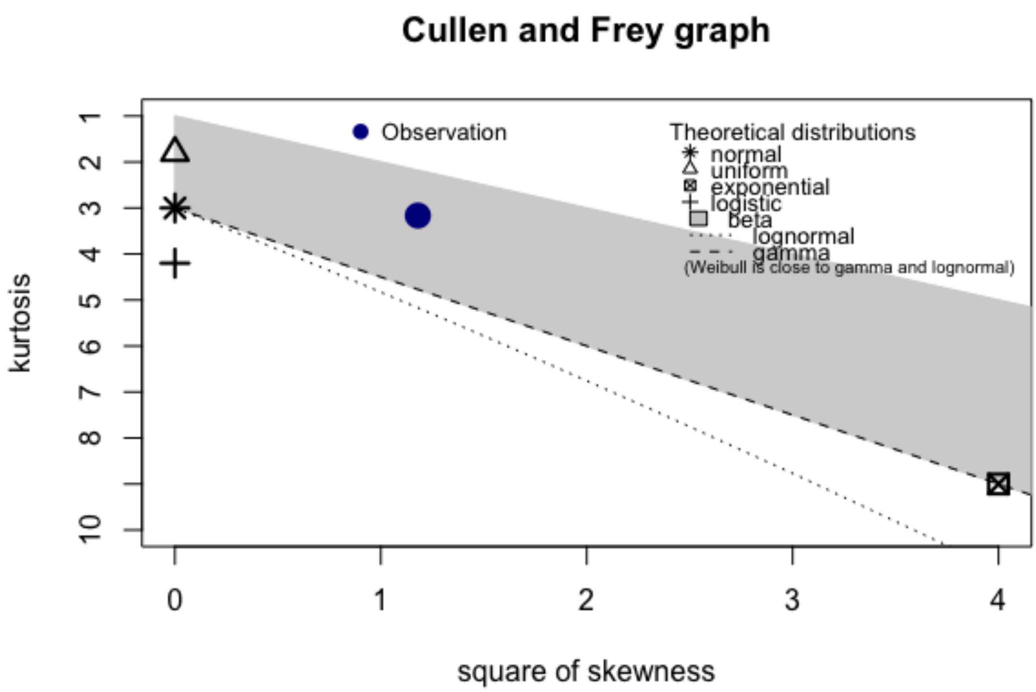

Appendix, figure 2. Cullen Frey Graph with theoretical distribution for the dependent variable before transformation. The observation is located in the Beta-distribution.

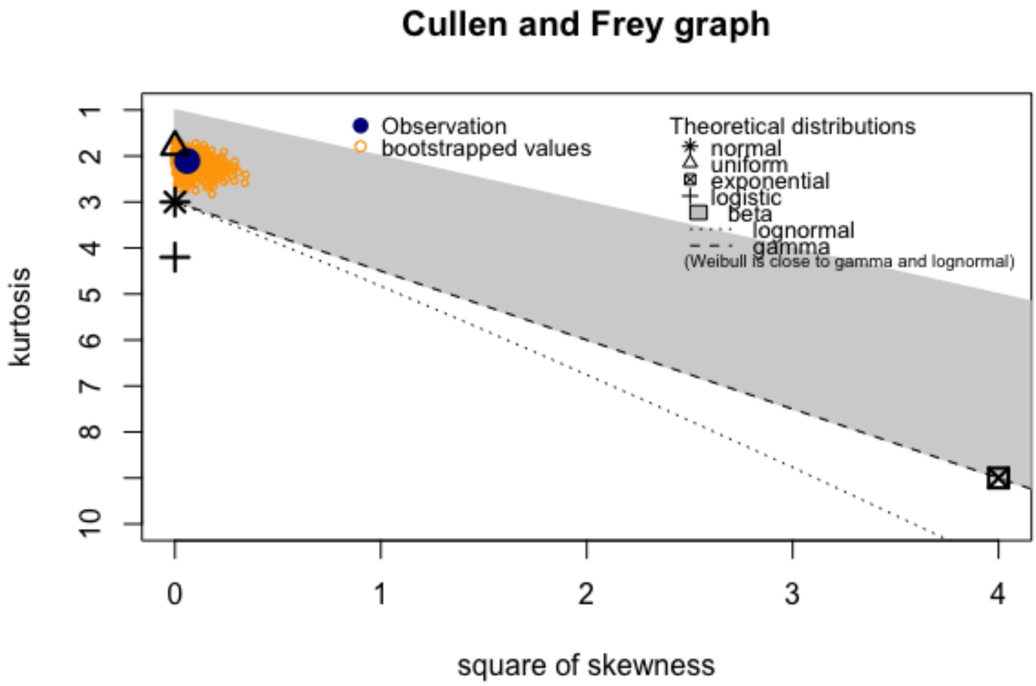

Appendix, figure 3. Cullen Frey Graph of the dependent variable after transformation. The formula included a bootstrap of 1,000. With the bootstrapped values, a linear regression could be suggested.

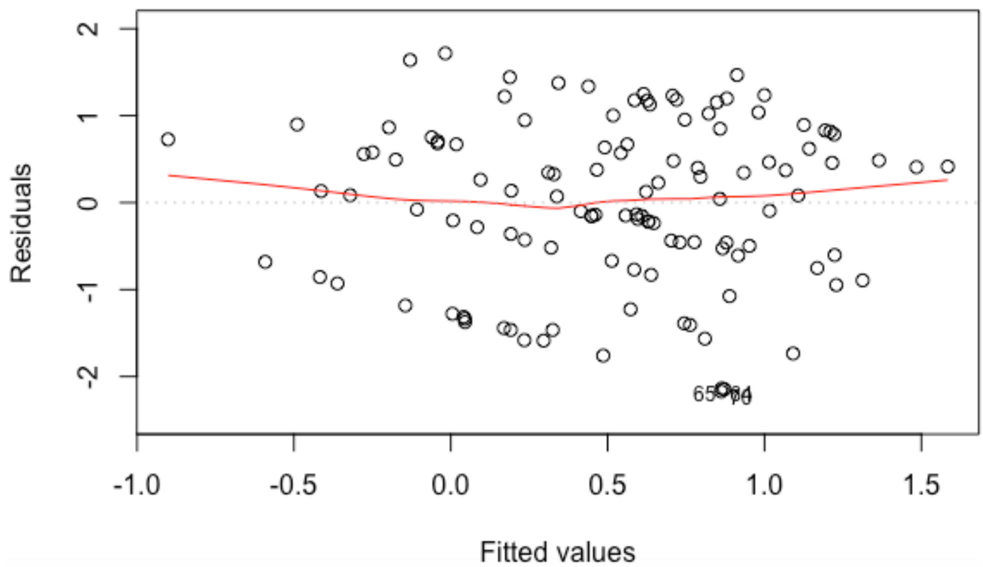

Appendix, figure 4. Residuals vs. Fitted. The line is somewhat horizontal. This figure was used in addressing the normality of the model.

Norges miljø- og biovitenskapelige universitet
Noregs miljø- og biovitskapelege universitet
Norwegian University of Life Sciences

Postboks 5003
NO-1432 Ås
Norway